


TESIS DOCTORAL

2018



**ESTUDIO DE LA INTERACCIÓN DE ELECTRONES
DE BAJA ENERGÍA (1-300 eV) CON
MOLÉCULAS DE INTERÉS BIOLÓGICO: *PARA-*
BENZOQUINONA, PIRIDINA, SEVOFLUORANO
Y TIOFENO**

ANA ISABEL LOZANO MARTÍNEZ

Director: GUSTAVO GARCÍA GÓMEZ-TEJEDOR

PROGRAMA DE DOCTORADO EN CIENCIAS

Tutora: AMALIA WILLIART TORRES

TESIS DOCTORAL

2018

ESTUDIO DE LA INTERACCIÓN DE ELECTRONES DE BAJA ENERGÍA (1-300 eV) CON MOLÉCULAS DE INTERÉS BIOLÓGICO: *PARA-* BENZOQUINONA, PIRIDINA, SEVOFLUORANO Y TIOFENO

ANA ISABEL LOZANO MARTÍNEZ

Trabajo realizado en el
**INSTITUTO DE FÍSICA FUNDAMENTAL
CSIC**

Bajo la dirección de
GUSTAVO GARCÍA GÓMEZ-TEJEDOR



Proyecto: FIS2016-80440



IFF

Agradecimientos

Hay muchas personas que han sido clave para que haya podido alcanzar este punto, la presentación de mi tesis doctoral, aquí quiero mencionar especialmente a algunos de ellos.

Ante todo, a Gustavo García, mi director de tesis. Gracias por haberme brindado la oportunidad de realizar esta tesis doctoral y sobre todo por haberme enseñado una vocación la cual aprecio y amo, la física experimental.

También agradecer a todos mis compañeros de laboratorio Mónica, Filipe, Lidia, Carlos, Ali, Lily y Kateryna. Vuestra ayuda ha sido fundamental para sobrellevar los días malos y para disfrutar de los logros alcanzados. En especial, Mónica Mendes, gracias por nuestras largas charlas las cuales nos han ayudado a resolver muchos problemas cotidianos en un laboratorio.

A María Dolores Gómez, mi profesora de Física en bachillerato, allá donde estés, gracias por creer en mí y haberme motivado, aunque diera algún que otro problema.

A aquellos que me han visto crecer y me han ayudado, siempre apoyando y creyendo, a aquellos...FAMILIA gracias.

A él, David

ÍNDICE

I. Compendio de trabajos publicados	1
II. Otros trabajos publicados relacionados con la presente tesis doctoral	2
III. Autorización del director	4
IV. Resumen	5
V. Abstract	6
VI. Informe tesis doctoral	7
VII. Publicaciones que conforma esta tesis doctoral	15
A. Pyridine	16
B. Sevoflurane	31
C. Thiophene	48
VIII. Lista completa de publicaciones	61

Compendio de trabajos publicados

La tesis presentada con título: “ESTUDIO DE LA INTERACCIÓN DE ELECTRONES DE BAJA ENERGÍA (1-300 eV) CON MOLÉCULAS DE INTERÉS BIOLÓGICO: PARA-BENZOQUINONA, PIRIDINA, SEVOFLUORANO Y TIOFENO” corresponde un compendio de trabajos previamente publicados. A continuación, se detalla para cada publicación: el título, los autores, la referencia completa de la revista o editorial y el DOI, así como el factor de impacto de la revista y el cuartil de esta según el Journal Citations Reports (JCR) en el momento de enviar los artículos a las revistas para su publicación.

“Total electron scattering cross section from pyridine molecules in the energy range 1-200 eV”

- *Autores:* Ana Isabel Lozano, Javier Jiménez, Francisco Blanco y Gustavo García
- *Referencia:* DOI: 10.1103/PhysRevA.98012709
- *Revista:* Physical Review A
- *Editorial:* American Physical Society
- *Factor de Impacto:* 2.925 (JRC-2016)
- *Cuartil:* Q2 (JCR-2016 *Physics, Atomic, Molecular & Chemical*)

“Total electron scattering cross section from sevoflurane by 1-300 eV energy electron impact”

- *Autores:* Ana Isabel Lozano, Filipe Ferreira da Silva, Francisco Blanco, Paulo Limão-Viera y Gustavo García
- *Referencia:* DOI: 10.1016/j.cplett.2018.07.005
- *Revista:* Chemical Physics Letters
- *Editorial:* Elsevier B. V.
- *Factor de Impacto:* 1.815 (JRC-2016)
- *Cuartil:* Q2 (JCR-2016 *Physics, Atomic, Molecular & Chemical*)

“Total electron scattering cross section from thiophene for the (1-300 eV) impact energy range”

- *Autores:* Ana Isabel Lozano, Alexandra Loupas, Francisco Blanco, Jimena D. Gorfinkiel y Gustavo García
- *Referencia:* DOI: 10.1063/1.5050349
- *Revista:* The Journal of Chemical Physics
- *Editorial:* AIP Publishing
- *Factor de Impacto:* 2.843 (JCR-2017)
- *Cuartil:* Q2 (JCR-2017 *Physics, Atomic, Molecular & Chemical*)

Otros trabajos publicados relacionados directamente con la presente tesis

A continuación, se enumeran otros trabajos publicados relacionados directamente con la presente tesis doctoral. Para cada uno, se detalla: el título, los autores, la referencia completa de la revista o editorial y el DOI, así como el factor de impacto de la revista y el cuartil de esta del Journal Citations Reports (JCR) en el momento de enviar los artículos a las revistas para su publicación.

“Low energy electron transport in furfural”

- *Autores:* Ana Isabel Lozano, Kateryna Krupa, Filipe Ferreira da Silva, Paulo Limão-Viera, Francisco Blanco, Antonio Muñoz, Darryl B. Jones, Michael J. Brunger y Gustavo García
- *Referencia:* DOI: 10.1140/epjd/e2017-80326-0
- *Revista:* European Physical Journal D
- *Editorial:* Springer
- *Factor de Impacto:* 1.288 (JCR-2016)
- *Cuartil:* Q3 (JCR-2016 *Physics, Atomic, Molecular & Chemical*)

“Magnetically confined electron beam system for high resolution electron transmission-beam experiments”

- *Autores:* Ana Isabel Lozano, Juan Carlos Oller, Kateryna Krupa, Filipe Ferreira da Silva, Paulo Limão-Viera, Francisco Blanco, Antonio Muñoz, Rafael Colmenares y Gustavo García
- *Referencia:* DOI: 10.1036/1.5030068
- *Revista:* Review of Scientific Instruments
- *Editorial:* AIP publishing
- *Factor de Impacto:* 1.515 (JCR-2016)
- *Cuartil:* Q3 (JCR-2016)

“Cross sections for electron scattering from thiophene for a broad energy range”

- *Autores:* Alexandra Loupas, Ana Isabel Lozano, Francisco Blanco, Jimena D. Gorfinkiel y Gustavo García
- *Referencia:* DOI: 10.1063/1.5040352
- *Revista:* The Journal of Chemical Physics
- *Editorial:* AIP Publishing
- *Factor de Impacto:* 2.843 (JCR-2017)
- *Cuartil:* Q2 (JCR-2017 *Physics, Atomic, Molecular & Chemical*)

“Total electron scattering cross sections from para-benzoquinone in the energy range 1-200 eV”

- *Autores:* Ana Isabel Lozano, Juan Carlos Oller, Darryl B. Jones, Romarly da Costa, Marcio T. Varella, Marcio H. Franco Bettega, Filipe Ferreira da Silva, Paulo Limão-Viera, Marco A. Lima, Ronald White, Michal B. Brunger, Francisco Blanco, Antonio Muñoz y Gustavo García
- *Referencia:* DOI: 10.1039/c8cp03297a

- *Revista:* Physical Chemistry Chemical Physics
- *Editorial:* Royal Society of Chemistry
- *Factor de Impacto:* 3.906 (JCR-2017)
- *Cuartil:* Q1 (JCR-2017 *Physics, Atomic, Molecular & Chemical*)

“Total cross section measurements for electron scattering from dichloromethane” (sometido a publicación)

- *Autores:* Ana Isabel Lozano, Lidia Álvarez, Francisco Blanco, Michael J. Brunger y Gustavo García
- *Referencia:*
- *Revista:* The Journal of Chemical Physics
- *Editorial:* AIP publishing
- *Factor de Impacto:* 2.843 (JCR-2017)
- *Cuartil:* Q2 (JCR-2017 *Physics, Atomic, Molecular & Chemical*)

Autorización del Director

Instituto de Física Fundamental (IFF)

Consejo Superior de Investigaciones Científicas (CSIC)

C/Serrano, 113-bis

28006, Madrid, España

Tel. +34 91 5616800, Exts. 943214-943207

Yo, Dr. Gustavo García Gómez-Tejedor con DNI: 00279548Y Investigador Científico en el **Instituto de Física Fundamental (IFF)** del Consejo Superior de Investigaciones Científicas (CSIC)

HAGO CONSTAR:

Que Ana Isabel Lozano Martínez, Licenciada en Física, ha realizado bajo mi dirección la Tesis Doctoral con título: **“ESTUDIO DE LA INTERACCIÓN DE ELECTRONES DE BAJA ENERGÍA (1-300 eV) CON MOLÉCULAS DE INTERÉS BIOLÓGICO: PARA-BENZOQUINONA, PIRIDINA, SEVOFLUORANO Y TIOFENO”** para optar al grado de doctora por la Universidad Nacional de Educación a Distancia (UNED). Así mismo, como director doy mi autorización para la presentación de dicha Tesis Doctoral y acepto la renuncia a usar cualquiera de los artículos que conforman el compendio de trabajos de dicha Tesis como parte otra Tesis Doctoral.

Y para que así conste, y tenga los efectos oportunos, firmo este certificado en Madrid, a 5 de
Noviembre del 2018



Resumen

En esta tesis, se presentan medidas experimentales novedosas de secciones eficaces totales de colisión de electrones de baja energía (1-300 eV) con moléculas de interés biológico en fase gaseosa: *para*-benzoquinona, piridina, sevoflurano y tiofeno. Para la realización de dichas medidas, se ha optimizado y validado un dispositivo experimental *estado del arte* basado en el transporte de electrones en condiciones de confinamiento magnético. La incertidumbre experimental asociada a todo el conjunto de datos presentados es $\leq 5\%$. Además, se ha proporcionado una estimación adecuada de un error sistemático inherente al aparato de medida derivado del confinamiento magnético del haz.

La validación del conjunto de datos experimentales que conforman esta tesis se ha realizado: Primero, a través de un análisis crítico de los resultados obtenidos y la comparación con otros resultados disponibles en la literatura, así como con los datos obtenidos a partir de los formalismos teóricos IAM-SCAR y *R*-matrix para el presente estudio; Segundo, mediante la simulación de un modelo de transporte de electrones basado en el método Monte Carlo.

Abstract

In this thesis, are reported on novel total cross sections measurements for low energy electrons (1-300 eV) scattering from molecular targets of biological interest in gas-phase: *para*-benzoquinone, pyridine, sevoflurane and thiophene. A *state of the art* apparatus, based on the magnetic confinement of the electron beam, has been optimized and validated to obtain the presented measurements. Random uncertainty limits on these values have been found to be $\leq 5\%$. In addition, a systematic error due to the magnetic confinement has been evaluated.

The set of experimental data which represent these thesis has been validated: Firstly, through a critical analysis of the obtained results and the comparison with other available data in the literature, as well as with calculated data derived from the IAM-SCAR and *R*-matrix methods carried out for the present study; Secondly, via an event-by-event Monte Carlo simulation based on the electrons transport.

INFORME TESIS DOCTORAL

CONTENIDO

1. Motivación	19
2. Hipótesis y objetivos planteados	19
3. Trabajos realizados	20
4. Conclusiones	22
5. Referencias	23

“If, in some cataclysm, all of scientific knowledge were to be destroyed, and only one sentence passed on to the next generations of creatures, what statement would convey the most information in the fewest words? I believe it is the atomic hypothesis (or the atomic fact) that all things are made of atoms- little particles that move around in perpetual motion, attracting each other when they are a little distance apart, but repelling upon being squeezed into one another.”
(Richard P. Feynman)

1. Motivación

El estudio de la interacción de electrones con moléculas biológicamente relevantes ha sido y sigue siendo objeto de numerosas investigaciones por parte de la comunidad científica internacional dada su relevancia en importantes aplicaciones dentro del campo de la medicina como la radioterapia, el radiodiagnóstico o la generación de nuevos medicamentos. Además, es crucial para profundizar en la comprensión de la actividad físico-química y la estructura de moléculas potencialmente interesantes a nivel biológico. El avance en estas aplicaciones demanda información exhaustiva acerca de todos los procesos inducidos por electrones en esas moléculas (excitaciones, ionización, captura electrónica, etc) y los parámetros de interacción de estos con las moléculas (secciones eficaces, tanto diferenciales como integrales) en el rango de energías más completo posible. En el caso de electrones de baja energía, esa información es crucial a la hora de estudiar el daño producido por radiación [1] o el transporte de electrones en plasmas [2]. Tal como se ha demostrado en trabajos anteriores [3], estos electrones juegan un papel decisivo en la rotura de enlaces de la molécula de ADN y por lo tanto en el daño inducido a nivel molecular.

Dentro de este marco, la sección eficaz total de colisión, TCS (del inglés “total scattering cross section”), es un parámetro clave ya que representa la suma de las contribuciones de todos los procesos que pueden tener lugar a una energía incidente dada. Así, medidas experimentales directas y precisas de TCS pueden ser usadas como valor de referencia para evaluar la consistencia de las secciones eficaces integrales parciales disponibles, ya sean calculadas o experimentales.

El trabajo desarrollado en esta tesis constituye una aportación de alto impacto en este campo de investigación dado que, (i) presenta medidas novedosas de secciones eficaces totales de colisión de electrones con moléculas de alto interés biológico, y (ii) las medidas han sido realizadas con un dispositivo experimental que cumple las exigencias del *estado del arte* actual en el campo de las colisiones electrónicas.

2. Hipótesis y objetivos a alcanzar

El objetivo general de esta tesis es estudiar la interacción de electrones de baja energía con moléculas de alto interés biológico con el fin de contribuir a la obtención de un conjunto de datos de secciones eficaces de colisión tan completo y autoconsistente como sea posible. Para ello, se plantearon los siguientes objetivos específicos a cumplir:

1. Optimización de un sistema experimental que cumpla con las exigencias del *estado del arte* actual.
2. Validación del sistema experimental con nitrógeno molecular (molécula de referencia) y diclorometano (molécula con momento dipolar no nulo).
3. Medida de secciones eficaces totales de colisión de electrones con moléculas de interés biológico en fase gaseosa en el margen de energías de 1 a 300 eV.

4. Verificación de los resultados obtenidos mediante la simulación de un modelo de transporte de electrones basado en el método Monte Carlo.

La consecución de estos objetivos se ha llevado a cabo de forma secuencial y se ha ido dejando constancia a través de la serie de publicaciones a las que ha dado lugar el presente trabajo:

- Primer y segundo objetivos:

A. I. Lozano, K. Krupa, F. Ferreira da Silva, P. Limão-Vieira, F. Blanco, A. Muñoz, D. B. Jones, M. J. Brunger, and G. García. "Low energy electron transport in furfural". *Eur. Phys. J. D* **71**, 226 (2017)

A. I. Lozano, J. C. Oller, K. Krupa, F. Ferreira da Silva, P. Limão-Vieira, F. Blanco, A. Muñoz, R. Colmenares, and G. García. "Magnetically confined electron beam system for high resolution electron transmission-beam experiments". *Rev. Sci. Instrum.* **89**, 063105 (2018)

A. I. Lozano, L. Álvarez, F. Blanco, M. J. Brunger, and G. García. "Total cross section measurements for electron scattering from dichloromethane". *J. Chem. Phys.* (sometido a publicación)

- Tercer objetivo:

A. I. Lozano, J. Jiménez, F. Blanco, and G. García. "Total electron-scattering cross section from pyridine in the energy range 1 -200 eV". *Phys. Rev. A* **98**, 012709 (2018)

A. I. Lozano, F. Ferreira da Silva, F. Blanco, P. Limão-Vieira, and G. García. "Total electron scattering cross section from sevoflurane by 1 – 300 eV energy electron impact". *Chem. Phys. Lett.* **706** (2018)

A. I. Lozano, A. Loupas, F. Blanco, J. D. Gorfinkiel, and G. García. "Total electron scattering cross sections from thiophene for the (1-300 eV) impact energy range". *J. Chem. Phys.* **149**, 134303 (2018)

- Cuarto objetivo:

Alexandra Loupas, **Ana I. Lozano**, Francisco Blanco, Jimena D. Gorfinkiel, and Gustavo García. "Cross sections for electron scattering from thiophene for a broad energy range". *J. Chem. Phys.* **149**, 034304 (2018)

A. I. Lozano, J. C. Oller, D. B. Jones, R. F. da Costa, M. T. do N. Varella, M. H. Bettega, F. Ferreira da Silva, P. Limão-Viera, M. A. P. Lima, R. D. White, M. J. Brunger, F. Blanco, A. Muñoz, and G. García. "Total electron scattering cross sections from *para*-benzoquinone in the energy range 1-200 eV". *Phys. Chem. Chem. Phys.* **20**, 22368 (2018)

3. Trabajos realizados

La presente tesis doctoral se ha realizado en el Instituto de Física Fundamental del Consejo Superior de Investigaciones Científicas. Los trabajos llevados a cabo durante el transcurso de la misma, han sido cronológicamente: el desarrollo y optimización de un dispositivo experimental de medida que cumpla con las exigencias del actual *estado del arte*, la validación de ese dispositivo, la medida de secciones eficaces totales de colisión de electrones con moléculas de interés biológico en fase gaseosa, el análisis crítico de los resultados obtenidos y la comparación con otros resultados disponibles en la bibliografía así como con cálculos teóricos realizados para este estudio, la preparación y discusión de los resultados obtenidos para su posterior publicación en revistas de impacto dentro del área de trabajo y finalmente, la

validación de las medidas experimentales obtenidas. A continuación, se presenta una breve descripción de las actividades realizadas dentro de cada una de estas etapas.

3.1. Dispositivo experimental

Se ha optimizado un dispositivo experimental ya existente basado en el transporte de electrones en condiciones de confinamiento magnético (en la dirección axial del haz de electrones) en gases moleculares en el rango de energías 1-300 eV [4]. Los primeros resultados obtenidos con ese dispositivo demostraron su falta de precisión en términos de resolución energética y angular por lo que la optimización ha consistido en la mejora de estos parámetros y de la precisión general del proceso de medida. Para ello, se han diseñado y construido tanto piezas mecánicas como circuitos electrónicos entre lo que destaca el diseño e implementación de una trampa magnética de gas para el enfriamiento del haz de electrones, nuevas lentes electrostáticas, nuevo diseño de las cámaras de interacción, mejora del sistema de aceleración y enfoque y finalmente el diseño de programas específicos para la adquisición y análisis de datos [5].

Para validar las medidas obtenidas con este dispositivo y corregir posibles errores sistemáticos asociados tanto al aparato como al proceso de medida, se ha medido la sección eficaz total de nitrógeno molecular (N_2) en el rango de energías 1-300 eV [5] y se ha comparado los resultados obtenidos con los valores de referencia disponibles en la literatura [6,7]. Posteriormente, para evaluar la magnitud de un error sistemático inherente al aparato de medida debido al confinamiento magnético del haz de electrones [5], el cual se ve incrementado para moléculas polares, se ha medido la sección eficaz total de una molécula con momento dipolar relativamente alto, diclorometano (CH_2Cl_2) [8]. Además, se ha propuesto un método para evaluar la magnitud de dicho error sistemático [5].

3.2. Medidas experimentales

Una vez validado el sistema experimental, se han medido secciones eficaces totales de colisión de electrones con moléculas de interés biológico en fase gaseosa en el margen de energías 1-300 eV. Las moléculas estudiadas se encuentran listadas en la Tabla I junto el rango energético en cada caso.

Para cada molécula estudiada, las medidas han sido realizadas siguiendo la misma metodología [5]. Además, antes de introducir un blanco nuevo, se ha medido la sección eficaz del nitrógeno molecular (N_2) para asegurar que no hubiera efectos de contaminación presentes, así como para contrastar el correcto funcionamiento del dispositivo experimental.

Para cada energía, los resultados se han obtenido utilizando la Ley de atenuación de Beer-Lambert, asumiendo un comportamiento de gas ideal de los blancos moleculares estudiados. Las medidas directas obtenidas tienen una reproducibilidad estadística $< 4\%$ y la incertidumbre experimental total asociada a ellas, una vez que se combinan todos los factores a tener en cuenta, es $\leq 5\%$ para todas las moléculas presentadas.

MOLECULE	ENERGY RANGE
piridina (C_5H_5N) ⁹	1 – 200 eV
sevoflurano ($C_4H_3F_7$) ¹⁰	1 – 300 eV
tiofeno (C_4H_4S) ¹¹	1 – 300 eV

Tabla I. Moléculas estudiadas para la presente tesis junto con el margen de energías considerado en cada caso.

3.3. Análisis de resultados

Se ha llevado a cabo un análisis crítico de los resultados que incluye, (i) cálculo de la resolución en energía del experimento, (ii) cálculo de la resolución angular asociada a la resolución energética dado el confinamiento magnético del haz de electrones [5], (iii) adaptación de los datos obtenidos mediante el cálculo IAM-SCAR+I [12-14] para su posterior comparación con los resultados experimentales obtenidos, (iv) búsqueda bibliográfica detallada para la realización de una discusión representativa y precisa en el contexto de otros datos publicados.

Una vez realizado lo anteriormente mencionado, se ha sintetizado toda la información en forma de artículo científico para su publicación en revistas de alto impacto dentro del campo de las colisiones electrón-molécula.

3.4. Validación de los resultados obtenidos

Un método eficiente para comprobar la validez de los datos de TCS experimentales es la simulación del transporte de electrones en los gases moleculares de interés utilizando el método Monte Carlo. Sin embargo, no es posible realizar este tipo de validación para cualquier molécula ya que para ello es necesaria una base de datos lo más completa posible que contenga todos los procesos inducidos por electrones y los parámetros de interacción de éstos con la molécula a modelar en el rango de energía de interés. Debido a la escasez de estos parámetros para las moléculas incluidas en esta tesis, se decidió hacer un estudio a posteriori sobre *para*-benzoquinona, *p*BQ [15]. Esta molécula fue elegida debido a su alto interés biológico y a la gran cantidad de secciones eficaces disponibles sobre ella.

Ese estudio ha servido: Primero, para evaluar la consistencia de las secciones eficaces disponibles usando como referencia las medidas experimentales de TCS obtenidas; segundo, para introducir esas secciones eficaces como parámetro de entrada en una simulación de transporte de electrones en *p*BQ y comparar con la distribución de intensidad observada experimentalmente. Por todo esto, este estudio se presenta como un anexo fundamental de este trabajo de investigación ya que da consistencia a la validez de los datos experimentales presentados que forman el cuerpo de esta tesis.

4. Conclusiones

En esta tesis, se ha realizado una investigación sobre la colisión de electrones con moléculas de alto interés biológico. Para ello, se han medido las secciones eficaces totales de colisión en el margen de energías 1-300 eV. Hasta donde sabemos, en el caso de la piridina, sólo podemos hablar de medidas obtenidas por primera vez para energías por debajo de 10 eV ya que en un estudio anterior llevado a cabo por Traoré-Dubuis *et al.* [15] se presentaron medidas de TCS de esta molécula en el rango de energías 10-1000 eV. Para el sevoflurano y tiofeno todo el conjunto de datos presentados es completamente novedoso.

Las medidas experimentales presentadas, han sido realizadas con un dispositivo experimental *estado del arte* que ha sido optimizado a partir de un prototipo usado en un estudio anterior sobre el transporte de electrones en furfural [4]. Este estudio fue clave para la identificación de mejoras a realizar en el dispositivo experimental, así como para identificar errores sistemáticos presentes y así poder corregirlos. Entre las mejoras realizadas, destaca el diseño e implementación de una trampa de gas lo cual ha llevado a alcanzar una resolución en energía del experimento de unos 200 meV.

Para cada molécula estudiada, las TCS experimentales han sido complementadas con las obtenidas mediante un cálculo realizado dentro del mismo grupo de investigación, utilizando el método IAM-SCAR+I. Este formalismo teórico ha sido extremadamente útil para la estimación adecuada del error sistemático inherente debido al confinamiento magnético del haz [5] a fin de lograr una comparación realista. Además, en todos los casos presentados se ha obtenido una correspondencia excelente entre ambos conjuntos de datos, teniendo en cuenta tanto el rango de validez del cálculo como la limitación angular del experimento. En el caso del tiofeno, el cálculo *R*-matrix [16], realizado por otro grupo de investigación para el presente estudio, ha resultado ser una potente herramienta para la discusión de los resultados en el margen de las energías más bajas. En los casos en que ha sido posible, se han comparado los presentes resultados experimentales con otros datos publicados, alcanzando un acuerdo excelente dentro de los límites de incertidumbre asignados. Por último, para dar consistencia a la validez del conjunto de datos experimentales que conforman esta tesis, se ha llevado a cabo un estudio con *para*-benzoquinona [15], en el que se ha podido comprobar que utilizando como parámetros de entrada las TCS experimentales de este trabajo, junto con valores complementarios de otras secciones eficaces, la simulación Monte Carlo de la distribución energética de los electrones transmitidos en dicho gas coincide con la que se observa experimentalmente.

Todo esto, nos lleva a concluir que los datos experimentales presentados en esta tesis, son datos novedosos y de gran relevancia dentro del campo de la interacción de electrones con moléculas de interés biológico. Los presentes valores, están en condiciones de ser añadidos al conjunto de bases de datos de secciones eficaces disponibles y pueden ser utilizados como valores de referencia en futuros estudios.

5. Referencias

- [1] A. G. Sanz, M. C. Fuss, A. Muñoz, F. Blanco, P. Limão-Viera, M. J. Brunger, S. J. Buckman, and G. García, *Int. J. Rad. Biol.* **88**, 71 (2012)
- [2] R. D. White, D. Cooks, G. Boyle, M. Casey, N. Garland, D. Konovalov, B. Philippa, P. Stokes, J. de Urquijo, O. González- Magaña, R. P. McEachran, S. J. Buckman, M. J. Brunger, G. García, S. Dujko, and Z. Lj. Petrovic, *Plasma Sources Sci. Technol.* **27**, 053001 (2018)
- [3] B. Boudaïffa, P. Cloutier, D. Hunting, M. A. Huels, and L. Sanche, *Science*, **287**, 1658 (2000)
- [4] A. I. Lozano, K. Krupa, F. Ferreira da Silva, P. Limão-Viera, F. Blanco, A. Muñoz, D. B. Jones, M. J. Brunger, and G. García, *Eur. Phys. J. D.* **71**, 226 (2017)
- [5] A. I. Lozano, J. C. Oller, K. Krupa, P. Limão-Viera, F. Blanco, A. Muñoz, R. Colmenares, G. García, *Rev. Sci. Instrum.* **89**, 063105 (2018)
- [6] C. Szmytkowski, and K. Maciag. *Phys. Scr.* **54**, 271 (1996)
- [7] Y. Itikawa, *J. Phys. Chem. Ref. Data* **35**, 31 (2006)
- [8] A. I. Lozano, L. Álvarez, F. Blanco, M. J. Brunger, and G. García, *J. Chem. Phys.* (sometido)
- [9] A. I. Lozano, J. Jiménez, F. Blanco, and G. García, *Phys. Rev. A* **98**, 012709 (2018)
- [10] A. I. Lozano, F. Ferreira da Silva, F. Blanco, P. Limão-Viera, and G. García, *Chem. Phys. Lett.* **706**, 533 (2018)
- [11] A. I. Lozano, A. Loupas, F. Blanco, J. D. Gorfinkiel, and G. García, *J. Chem. Phys.* **149**, 134303 (2018)
- [12] F. Blanco, J. Rosada, A. Illana, and G. García, *Phys. Lett. A* **374**, 4420 (2010)
- [13] F. Blanco, L. Ellis-Gibbins, and G. García, *Chem. Phys. Lett.* **645**, 71 (2015)
- [14] A. Traoré Dubuis, A. Verkhovtsev, L. Ellis-Gibbins, K. Krupa, F. Blanco, D. B. Jones, M. J. Brunger, and G. García, *J. Chem. Phys.* **147**, 054301 (2017)
- [15] A. I. Lozano, J. C. Oller, D. B. Jones, R. F. da Costa, M. T. do N. Varella, M. H. Bettega, F. Ferreira da Silva, P. Limão-Viera, M. A. P. Lima, R. D. White, M. J. Brunger, F. Blanco, A. Muñoz, and G. García, *Phys. Chem. Chem. Phys.* **20**, 22368 (2018)

[16] A. Loupas, A. I. Lozano, F. Blanco, J. D. Gorfinkield, and G. García, *J. Chem. Phys.* **149**, 034304 (2018)

Publicaciones que conforman la presente tesis doctoral

A. "Total electron scattering cross section from **pyridine** molecules in the energy range 1 – 200 eV"

B. "Total electron scattering cross section from **sevoflurane** by 1 – 300 eV energy electron impact"

C. "Total electron scattering cross sections from **thiophene** for the (1 – 300 eV) impact energy range"

Total electron-scattering cross sections from pyridine molecules in the energy range 1–200 eVA. I. Lozano,^{1,2} J. Jiménez,¹ F. Blanco,³ and G. García^{1,4,*}¹*Instituto de Física Fundamental, Consejo Superior de Investigaciones Científicas, 28006 Madrid, Spain*²*Escuela de Doctorado de la UNED-Programa de Doctorado en Ciencias, 28015 Madrid, Spain*³*Departamento de Física Atómica, Molecular y Nuclear, Universidad Complutense de Madrid, 28040 Madrid, Spain*⁴*Centre for Medical Radiation Physics, University of Wollongong, NSW, Australia*

(Received 30 April 2018; published 17 July 2018)

We report on total electron-scattering cross sections from pyridine as measured with a magnetically confined electron-beam system for impact energies ranging from 1 to 200 eV, including measurements for energies below 10 eV. Reasonable agreement with previous measurements for energies above 10 eV has been found. Systematic errors arising from elastically and rotationally scattered electrons into the detector acceptance angle have been evaluated. Results are compared with available calculation both for the 10–200 eV and below 10 eV energy ranges. The evaluated data provided in this study will facilitate electron transport modeling in biologically relevant media.

DOI: [10.1103/PhysRevA.98.012709](https://doi.org/10.1103/PhysRevA.98.012709)**I. INTRODUCTION**

In the last decade, the need to understand microscopic radiation damage in biomolecular systems [1] has motivated numerous theoretical and experimental electron-scattering cross-section (CS) studies for biologically relevant molecules [2]. These data are needed to model radiation interactions with biological media [1] when accurate description of both energy deposition and induced molecular dissociation are required [3]. Pyridine has been considered a prototypical molecule for DNA bases and consequently it has received considerable attention in the last few years [4,5]. The total electron-scattering cross sections (TCSs) are an important parameter for checking the consistency of the collisional database available for a given molecular target. They represent the sum of the partial cross-section contributions from all scattering channels which are open at a given energy and therefore they are used as reference values to evaluate the completeness of a data set. In the case of pyridine, we have recently published experimental TCS values [6] for impact energies ranging from 10 to 1000 eV as measured with a double-spectrometer transmission-beam technique, together with an update of our previous Independent Atom Model with the Screening Corrected Additivity Rule (IAM-SCAR) calculation [5] by incorporating the effect of interferences in the elastic scattering cross sections (IAM-SCAR+I) [7]. Although those experimental results confirmed the reliability of the updated calculation by showing better agreement when interference terms are included, they are systematically lower than the calculated results, suggesting that new measurements with different techniques should be carried out to identify possible systematic errors. In addition, scattering resonances predicted by the available calculations below 10 eV [4,5] require experimental validation. Scattering of charged particles from polar molecules presents great difficulty both from the theoretical and experimental points of view. Even for one of the most well-studied molecules, water, great discrepancies

remain between the total cross sections for low-energy electrons [8] and positrons [9] when results are compared between different theoretical and experimental sources. Pyridine possesses a relatively high permanent dipole moment (~ 2.2 D [10]) and as such the lower-energy scattering is dominated by dipole interactions, therefore requiring greater detail when comparing results from different theoretical and experimental techniques to overcome this complication.

These considerations motivated the present experimental study, in which total electron-scattering cross sections from pyridine are measured using a state of the art magnetically confined transmission-beam technique [11]. This experimental system incorporates a nitrogen trap to cool the electron beam before entering the scattering region, providing accurate TCS measurements with random uncertainty limits within 5%.

The experimental technique and measurement procedures are described in Sec. II together with a detailed analysis of the possible uncertainty sources that may affect the present measurements. Results are presented in Sec. III and compared with available theoretical and experimental data. Finally, some concluding remarks are presented in Sec. IV.

II. EXPERIMENTAL SETUP AND MEASUREMENT PROCEDURE

The experimental system has been presented in detail in a previous article [11]; hence here we give only a brief description.

A schematic diagram of the experimental setup is shown in Fig. 1. The electron-beam line is divided into four sections: electron gun (EG), gas trap (GT), interface chamber (IC), scattering chamber (SC), and detector area (AD). The latter three are mutually separated by differential pumping and all sections of the experimental systems are surrounded by solenoids, generating axial magnetic fields of different intensities.

The primary electron beam is generated through thermionic emission by a tungsten filament, then extracted, collimated, and accelerated into the 60-mm-length nitrogen cooling trap.

*g.garcia@csic.es

Total electron scattering cross sections from pyridine molecules in the energy range 1-200 eV.

A. I. Lozano,^{1,2} J. Jiménez,¹F. Blanco,³and G. García^{1,4*}

¹*Instituto de Física Fundamental, Consejo Superior de Investigaciones Científicas, 28006 Madrid, Spain*

²*Escuela de Doctorado de la UNED-Programa de Doctorado en Ciencias, 28015 Madrid, Spain*

³*Departamento de Física Atómica, Molecular y Nuclear, Universidad Complutense de Madrid, 28040 Madrid, Spain*

⁴*Centre for Medical Radiation Physics, University of Wollongong, NSW, Australia*

We report on total electron scattering cross sections from pyridine as measured with a magnetically confined electron-beam system for impact energies ranging from 1 to 200 eV, including the first reported measurements for energies below 10 eV. Reasonable agreement with previous measurements for energies above 10 eV has been found. Systematic errors arising from elastically and rotationally scattered electrons into the detector acceptance angle have been evaluated. Results are compared with available calculation both for the 10-200 eV and below 10 eV energy ranges. The evaluated data provided in this study will facilitate electron transport modelling in biologically relevant media.

I. INTRODUCTION

In the last decade, the need to understand microscopic radiation damage in biomolecular systems [1] has motivated numerous theoretical and experimental electron scattering cross section (CS) studies for biologically relevant molecules [2]. These data are needed to model radiation interactions with biological media [1] when accurate description of both energy deposition and induced molecular dissociation are required [3]. Pyridine has been considered a prototypical molecule for DNA bases and consequently it has received considerable attention in the last few years [4, 5]. The total electron scattering cross sections (TCS) are an important parameter to check the consistency of the collisional data base available for a given molecular target. They represent the sum of the partial cross section contributions from all scattering channels which are open at a given energy and therefore they are used as reference values to evaluate the completeness of a data set. In the case of pyridine, we have recently published

* g.garcia@csic.es

experimental TCS values [6] for impact energies ranging from 10 to 1000 eV as measured with a double spectrometer transmission-beam technique, together with an update of our previous IAM-SCAR calculation [5] by incorporating the effect of interferences in the elastic scattering cross sections (IAM-SCAR+I) [7]. Although those experimental results confirmed the reliability of the updated calculation by showing better agreement when interferences terms are included, they are systematically lower than the calculated, suggesting that new measurements with different techniques should be carried out to identify possible systematic errors. In addition, scattering resonances predicted by the available calculations below 10 eV [4, 5] require experimental validation. Scattering of charged particles from polar molecules presents great difficulty both from the theoretical and experimental points of view. Even for one of the most well-studied molecules, water, great discrepancies remain between the total cross sections for low energy electrons [8] and positrons [9] when results are compared between different theoretical and experimental sources. Pyridine possesses a relatively high permanent dipole moment (~ 2.2 D [10]) and as such the lower energy scattering is dominated by dipole interactions, therefore requiring greater detail when comparing results from different theoretical and experimental techniques to overcome this complication.

These considerations motivated the present experimental study, in which total electron scattering cross sections from pyridine are measured using a state of the art magnetically confined transmission beam technique [11]. This new experimental system incorporates a nitrogen trap to cool the electron beam before entering the scattering region, providing accurate TCS measurements with random uncertainty limits within 5%.

The experimental technique and measurement procedures are described in Section II together with a detailed analysis of the possible uncertainty sources that may affect the present measurements. Results are presented in Section III and compared with available theoretical and experimental data. Finally, some concluding remarks are presented in Section IV.

II. EXPERIMENTAL SETUP AND MEASUREMENT PROCEDURE

The experimental system has been presented in detail in a previous article [11], hence here we give only a brief description.

A schematic diagram of the experimental setup is shown in Fig. 1. The electron beam line is divided into four sections: electron gun (EG), gas trap (GT), interface chamber (IC), scattering chamber (SC) and detector area (AD). The latter three are mutually separated by differential pumping and all sections of the experimental systems are surrounded by solenoids, generating axial magnetic fields of different intensities.

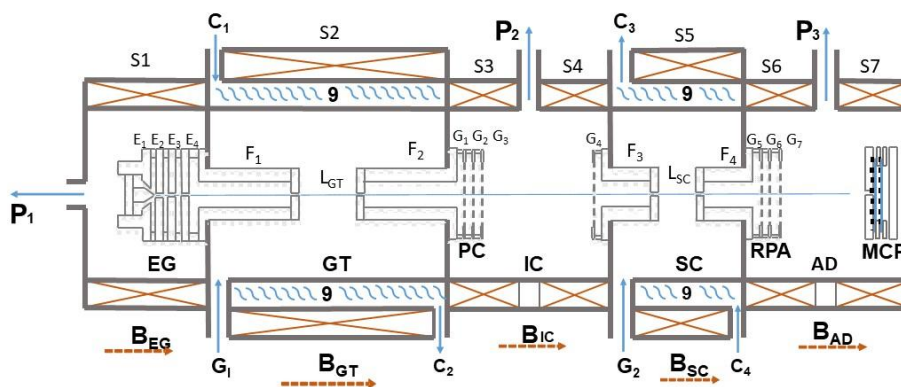


FIG. 1. Schematic diagram of the experimental setup; EG, electron gun; GT, gas trap; IC, interphase chamber; PC, pulse-controlling system; SC, scattering chamber; RPA, retarding potential analyser; AD, detection area; MCP, microchannel plate detector; P_1 , P_2 , P_3 , differential pumping system; B_{EG} , B_{GT} , B_{IC} , B_{SC} , B_{AD} , axial magnetic fields of the different chambers generated by the corresponding solenoids (S_1 - S_7); C_1 , C_2 , C_3 , C_4 , water cooling system; G_1 , G_2 , gas inlet to the GT and SC, respectively. (See also text for further explanation)

The primary electron beam is generated through thermionic emission by a tungsten filament, then extracted, collimated and accelerated into the 60 mm length nitrogen cooling trap. Here its energy spread is reduced down to about 200 meV by successive collisions with the cooling gas (N_2). The kinetic energy along the gas trap, around 7 eV, was optimised to balance the transmitted electron intensity and the effective cooling via vibrational and electronic excitation of the N_2 molecules. At the exit of the gas trap a three grid system (PC) is used to pulse and control the electron beam. The axial magnetic field inside the gas trap (B_{GT}) was typically within 0.05-0.1 T. As described in Ref. [11] under these axial magnetic confinement conditions, any collision event in the GT chamber converts the expected scattering angle (θ) into a kinetic energy loss in the direction parallel to the beam ($E_{||}$), according to $E_{||} = E \cos^2 \theta$, E being the incident kinetic energy. The scattering chamber (SC) has a similar geometry but it is 40 mm in length and the three grid element at the exit constitutes a retarding potential energy analyser (RPA). Pyridine is introduced into the SC through a leak valve and maintained to a constant pressure which was varied between 0 and 3 mTorr during the measurements. The target gas

pressure was measured with an MKS Baratron (627B) capacitance manometer. Electrons transmitted through the RPA are finally detected by a two stage microchannel plate operating in single pulse counting conditions. The kinetic energy of incident electrons in the SC is determined by $E = e|V_{GT}-V_{SC}|$, V_{GT} and V_{SC} being the potentials applied to the GT and SC, respectively. In this way the scattering energy is varied while still maintaining nitrogen cooling of the electron beam. The axial magnetic field inside the SC (B_{SC}) was 0.05-0.1 T in order to ensure magnetic confinement conditions [11]. The role of the remaining magnetic fields (B_{EG} , B_{IC} and B_{AD}) is simply to guide the beam between chambers and their intensities were optimised for each energy studied to maximise transmission while maintaining the energy resolution. The different stages are differentially pumped reaching background pressures of the order of 10^{-8} Torr and maintained below 10^{-6} Torr in the EG, IC and AD stages during operation. Maximum GT and SC operating pressures were 60 and 3 mTorr respectively.

Total cross sections are determined by the attenuation of the incident electron beam passing through a scattering chamber containing a well-known density of the molecular target according to the Lambert-Beer law:

$$I = I_0 e^{-n\sigma_T L} \quad (1)$$

Where I is the transmitted electron intensity, I_0 the initial intensity, n the molecular gas density, σ_T the total cross section and L the interaction length. Assuming an ideal gas, this equation can be rewritten as:

$$\ln\left(\frac{I}{I_0}\right) = -\frac{L\sigma_T}{kT} p, \quad (2)$$

where k is Boltzmann's constant, T is the absolute temperature and p is the gas pressure. T is derived from $T = \sqrt{T_c T_m}$, where T_c and T_m are the temperature of the scattering chamber measured with a thermocouple and the Baratron gauge operating temperature. According to the above procedure, a semi-logarithmic plot of Eq. (2) as a function of p can produce σ_T by simple slope (m) analysis, as follows:

$$\sigma_T = \frac{mkT}{L}. \quad (3)$$

In this way the electron transmission/attenuation as a function of pressure through a gas is able to provide TCS data.

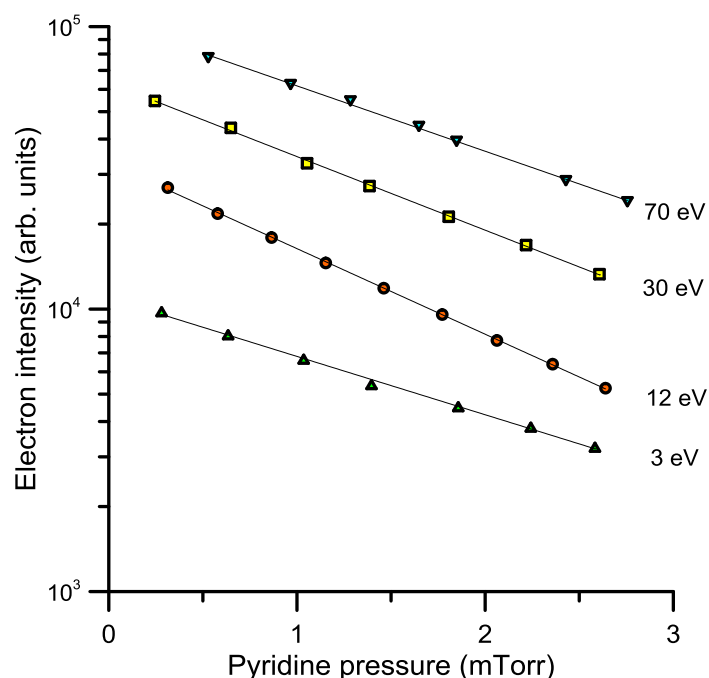


FIG. 2. Attenuation curves as a function of pyridine pressure for different impact energies.

Typical attenuation curves for different incident energies are shown in Fig.2. As can be seen in the figure, single exponential functions can be used to fit all energies for the pressures used (1-3 mTorr), indicating multiple scattering processes are excluded from these measurements. Accurate values of the slope m can as such be determined to produce precise TCS data. For each incident electron energy, attenuation measurements were repeated at least 5 times to ensure that statistical uncertainties remained below 4%. Other random uncertainties are linked to the temperature measurement (within 1%, according to manufacturer's data) and the numerical fitting procedure (about 1%). By individually calculating these uncertainties for each incident energy, a random uncertainty maximum of 5 % has been determined for the present measurements.

Possible systematic errors have been investigated in previous benchmarking measurements for molecular nitrogen [11]. Under the present experimental conditions space charge and multiple scattering effects are insignificant, evidenced by no dependence of the measured TCS values on electron current or gas pressure. In addition, the excellent agreement found for N_2 as compared with available reference data [12, 13] indicates that the real interaction length coincides with the geometrical SC length and that the assumed magnetically confined conditions [11] are properly representing the scattering processes within the considered energy range. The magnetic confinement does produce an inherent systematic error in this technique, linked to the relationship between the angular resolution ($\Delta\theta$) and the energy resolution (ΔE), which is affecting the present measurements. As explained in Ref. [11], within the intense axial magnetic

field, for elastic and rotational excitation collisions, the energy transferred to the target is negligible but the expected deflection (θ) of the scattered electron is converted into an energy loss (ΔE) in the direction of the axial magnetic field ($E_{||}=E \cos^2 \theta$). Obviously $\Delta E= E- E_{||}$ and therefore the minimum scattering angle resolved ($\Delta \theta$) is linked to the energy resolution of the detector through the following expression (see Ref. [11] for details):

$$\Delta \theta = \arccos \sqrt{1 - \frac{\Delta E}{E}} \quad (4)$$

Those electrons elastically or rotationally inelastically scattered into the $\Delta \theta$ angle are considered by the detector as unscattered, lowering the measured TCS. The magnitude of this systematic error, $\sigma(\Delta \theta)$ can be evaluated from theoretical data by integrating the calculated differential cross sections over the missing experimental angles:

$$\sigma(\Delta \theta) = 2\pi \left(\int_0^{\Delta \theta} \frac{d(\sigma_{el} + \sigma_{rot})}{d\Omega} \sin \theta d\theta + \int_{180-\Delta \theta}^{180} \frac{d(\sigma_{el} + \sigma_{rot})}{d\Omega} \sin \theta d\theta \right), \quad (5)$$

where σ_{el} and σ_{rot} represent the elastic and rotational cross sections, respectively. Depending on the target, vibrational excitation energies of the ground state may be lower than ΔE and so contribute to the $\sigma(\Delta \theta)$ term. Differential vibrational excitation cross sections from pyridine are not available in the literature but similar data for pyrimidine [3] indicate that the vibrational contribution to the angular resolution systematic error can be neglected. Calculated DCS can be used to evaluate the magnitude of the above systematic error. The main contribution to this uncertainty is due to the electron scattered into the experimental acceptance angles by rotational excitation processes. This situation is illustrated in Fig. 3, showing how for small scattering angles, below 1° , the rotational excitation DCS increment its value more than 5 orders of magnitude when the incident electron energy is 10 eV. Note that more than 90% of this systematic error is due to the rotational excitation cross sections which are not discernible for most of the experiments and their calculated values mostly rely on the Born approximation [5].

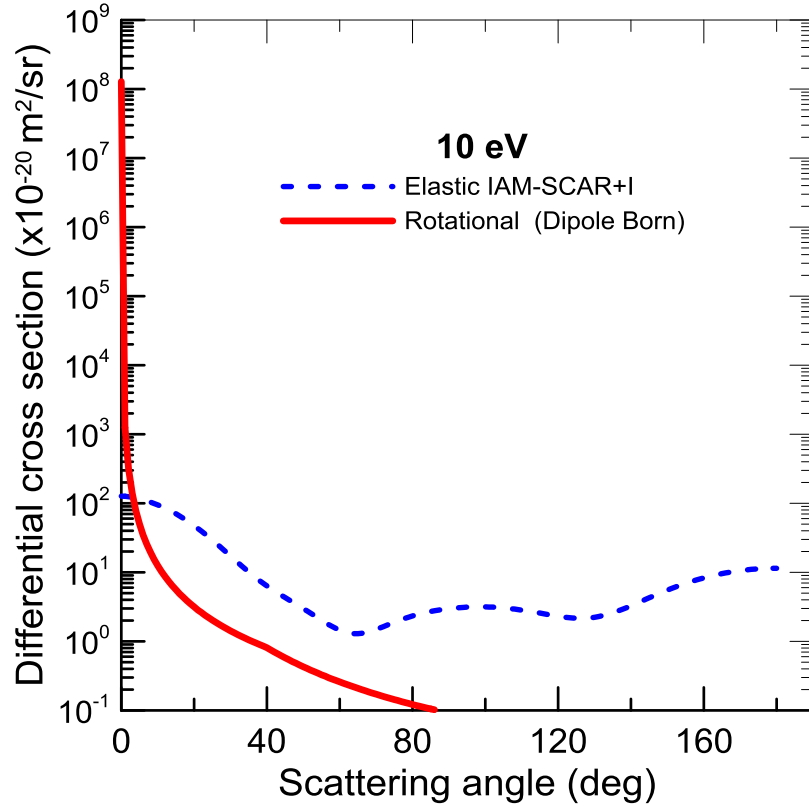


FIG. 3 Differential elastic cross section calculated with the present IAM-SCAR+I method and the differential rotational excitation cross sections derived from Born approximation (see Ref. [5] for details)

II. RESULTS AND DISCUSSION

The present experimental TCS with their absolute random uncertainty limits are shown in Table 1. The energy resolutions and the corresponding angular resolutions (Eq. 4) are also shown in this table for each incident energy. The later can be used to determine the aforementioned systematic error by using the appropriate DCS values.

Table 1. Present experimental electron scattering cross sections indicating their random uncertainty limits, the energy resolution and the acceptance angle of the detector.

Energy (eV)	Total cross section ($\times 10^{-20} \text{ m}^2$)	Absolute random uncertainty limit ($\times 10^{-20} \text{ m}^2$)	Energy resolution (ΔE , in eV)	Acceptance angle ($\Delta\theta^\circ$)
1	36.8	0.87	0.22	27.9
1.2	39.2	0.57	0.23	25.9
1.5	35.4	1.1	0.22	22.5
1.7	31.5	0.67	0.23	21.6
2	30.4	1.2	0.23	19.8

2.3	34.7	1.5	0.23	18.4
2.6	37.1	1.4	0.23	17.3
2.8	38.7	1.3	0.23	16.6
3	40.3	1.5	0.20	14.9
3.2	37.8	1.0	0.21	14.8
3.5	34.6	1.2	0.22	14.5
3.7	38.7	1.2	0.20	13.4
4	44.1	1.9	0.23	13.8
4.2	49.1	2.1	0.23	13.5
4.4	51.3	1.1	0.23	13.2
4.6	53.6	2.0	0.23	12.9
4.8	51.7	1.2	0.23	12.6
5	49.6	1.6	0.23	12.4
5.2	45.2	1.9	0.23	12.1
5.5	47.8	1.3	0.22	11.5
5.8	50.2	1.5	0.22	11.2
6	50.1	2.4	0.22	11.0
6.5	53.7	0.90	0.22	10.6
7	57.8	2.2	0.22	10.2
7.5	55.1	1.6	0.21	9.63
8	55.7	2.3	0.20	9.10
8.5	60.4	2.6	0.20	8.82
9	58.7	2.0	0.22	8.99
9.5	58.8	1.1	0.20	8.34
10	60.3	2.2	0.19	7.92
11	58.9	2.9	0.24	8.49
12	55.1	1.7	0.23	7.96

13	51.1	1.7	0.27	8.29
14	55.6	1.7	0.19	6.69
15	54.4	2.6	0.19	6.46
16	52.3	1.6	0.20	6.42
17	51.4	0.79	0.20	6.23
20	50.9	2.4	0.22	6.02
25	50.9	1.7	0.22	5.38
30	48.2	1.6	0.22	4.91
40	45.9	1.4	0.22	4.25
50	44.3	1.3	0.20	3.63
70	39.9	0.91	0.22	3.21
90	37.7	0.61	0.18	2.56
100	36.2	1.2	0.24	2.81
150	29.3	0.65	0.24	2.29
200	24.3	0.87	0.24	1.98

To our knowledge, the only experimental TCS data available in the literature are those obtained by Traoré-Dubuis *et al.* [6] using a double spectrometer transmission beam technique. In the overlapping energy domain (13-174 eV), present results are slightly higher than those of Ref. [6] but the differences are less than 12%, so they are technically in agreement within the combined uncertainty limits. This difference cannot be explained by the better angular resolution (0.25° acceptance angle) used in Ref. [6] which would act in the opposite direction. We therefore could speculate that the possible pressure gradients mentioned in Ref. [6] are still affecting their results. An important motivation for measuring accurate TCSs is to check the consistency of the recently incorporated interference effects [7] to our IAM-SCAR calculation [5]. The significant permanent dipole moment (2.2 D [10]) of pyridine complicates this comparison at the elastic scattering level, especially for the lower energies where dipole rotational excitations are dominant. In addition, both interference effects and dipole interactions tend to preferentially scatter electrons in the forward direction, increasing the acceptance angle error of the experimental system. The experimental results are compared to literature data from three

calculation methods: the integral elastic, inelastic and total cross sections given by the IAM-SCAR+I [6] procedure and the rotationally summed integral elastic cross sections derived from the Schwinger multichannel (SMC) [4] and the R-matrix [5] methods. All three use the fixed nuclei representation, hence to include dipole interactions some corrections based on the Born approximation need to be implemented. In IAM-SCAR+I these take the form of approximated rotational cross sections, becoming the IAM-SCAR+I+R method. These approximated rotational excitation cross sections are in general less accurate than the respective original calculation methods and present some difficulties in reproducing the temperature dependent initial rotational state distributions of the experimental targets. Keeping in mind these considerations a comparison between the experimental and theoretical results is plotted in Fig. 4.

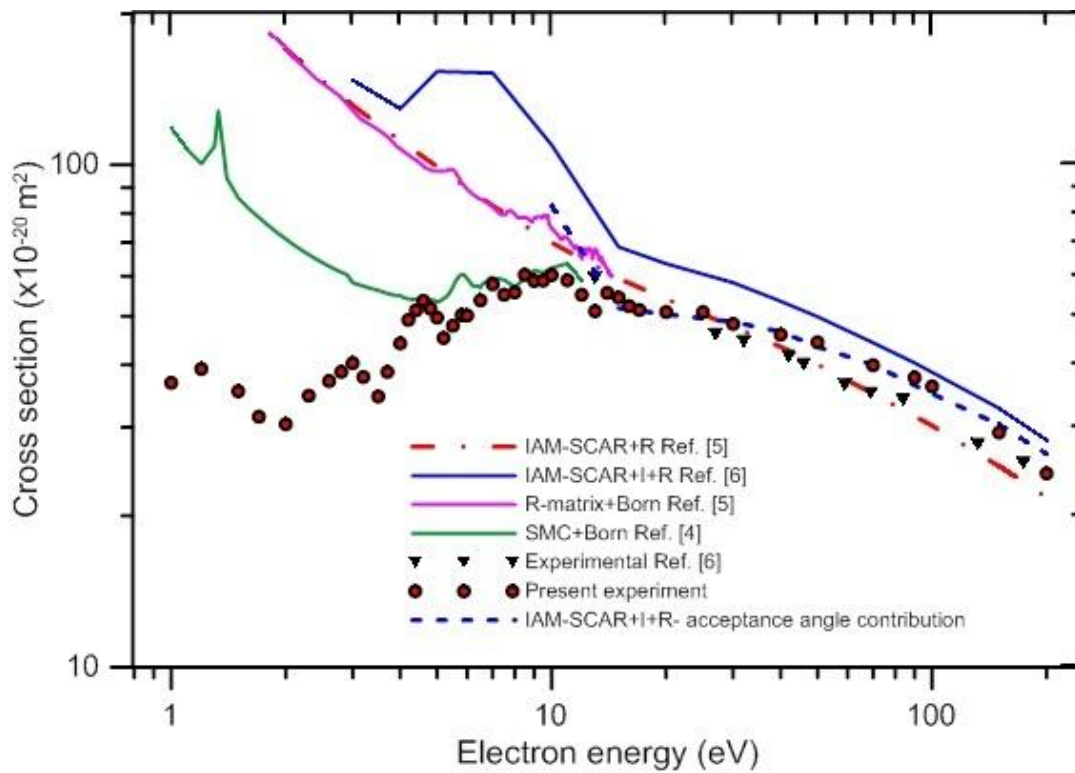


FIG. 4. Rotationally summed integral elastic cross sections calculated in refs. [4] and [5], total electron scattering cross sections calculated in refs. [5] and [6] with and without acceptance angle corrections and present electron scattering cross section measurements (see also legend for symbols and text for details).

Comparing the present experimental TCSs with those calculated with our IAM-SCAR+I+R [6] method, the theoretical values are generally higher than the experimental by 10-25% for impact energies above 10 eV. Below 10 eV the IAM-SCAR approximation [14, 15] does not apply and we can only expect a qualitative estimate. For this reason, we are not including in this comparison the IAM-SCAR data below 10 eV. In this energy domain, a more sophisticated description of the molecular wave functions and the scattering equation is required to obtain suitable cross section values and account for resonances. If we compare our experimental results with the Born

corrected SMC calculation from Ref. [4], the experimental data are in general lower in magnitude. As the calculations include rotational excitation and the measurements do not account for them, comparison between the absolute values does not make sense but the position of the resonances can be discussed. Note that below 2.5 eV, they agree well on the position of a low-lying resonance. Earlier theoretical studies from Mašín et al. [16] predicted four π^* shape resonances in electron collisions with diazines. However, in the case of pyridine (azine) Sieradzka et al. [5] only found three π^* resonances. The SMC calculation for pyridine from Ref. 4, in the energy range considered in this study, identifies resonances at 1.33 eV which can be classified as 2A_2 (see Refs. 4, 5) and another 2B_1 at 5.90 eV.

Our experimental results show a resonance at 1.2 ± 0.2 eV, which is in agreement with the 2A_2 calculated by Barbosa et al [4]. We can also distinguish a resonance at 4.6 ± 0.2 eV which is about 1.3 eV lower in energy than the 2B_1 given in Ref. [4], but in perfect agreement with the 4.58 eV shape resonance experimentally identified by Nenner and Schultz [17]. In addition, Modelli and Burrow [18] studying temporary anion formation in pyridine with an electron-transmission technique found this resonance at 4.48 eV, in agreement with the present result within experimental uncertainty. The R-matrix calculation from Ref. [5] also predicts well the position of the 2A_2 resonance at 1.07 eV, but gives an energy position for the 2B_1 which is 16% higher in energy than the present experimental value.

The R-matrix integral elastic cross sections (IECS) [5] with the equivalent SMC results [4] (both rotationally summed and Born corrected) clearly differ. Initial discrepancies between the non-Born corrected results were discussed in Ref. [5]. These were attributed to the different basis sets used by the two methods and the treatment of the long range polarisation interaction, which is not considered in the external R-matrix sphere [5]. The Born correction procedure to include the higher order partial waves in the calculation was essentially the same in both methods, based on the original formulation of Lucchese and Gianturco [19]. However, the R-matrix [5] IECS values are about factor 2 higher in magnitude than the SMC for impact energies below 5 eV. As mentioned above, at energies below 10 eV, where the independent atom approximation fails, it does not make sense to compare experiment with the IAM-SCAR+I+R calculation. However, it is interesting to note the different method with which the latter incorporates rotational excitations. While R-matrix and SMC methods consider the target molecule in its ground rotational state before the collision, the IAM-SCAR+I+R assumes a thermal distribution of the initial J -rotational states [20] accessible at room temperature and then calculates $\Delta J = \pm 1$ transitions within the framework of the Born approximation [21], including the Dickinson correction [22] for large scattering angles. For energies above 10 eV, the

reliability of this representation is shown by the good agreement in Fig. 4 between the present experimental data and the IAM-SCAR+I+R calculation when the aforementioned $\sigma(\Delta\theta)$ correction, which is mainly due to rotational excitations, is subtracted from the calculated TCSs. The effect of this subtraction within the energy range from 10 to 200 eV is lowering the calculated TCSs from 25 to 6%, respectively.

In addition, between 2.2 and 3.5 eV we obtained a resonant-type cross section increase, not seen in either calculation, with a local maximum at 3.0 ± 0.2 eV. This may be attributed to the excitation of an inelastic channel not included in the respective calculations. Considering the experimental energy loss study of Walker *et al.* [24], no electronic excitation peak appears around that energy. We can therefore assign this peak to the vibrational excitation of the ground state. No data was found in the literature on vibrational excitation of pyridine by electron impact but a compilation of vibrational excitation cross sections of pyrimidine [25] exists. This showed that vibrational excitations of the ground state for this molecule present a prominent maximum in cross section of about $10 \times 10^{-20} \text{ m}^2$ at a collision energy of 4 eV, which is compatible with the increase on the cross section we measured for pyridine around 3 eV. The next cross section increase begins at 3.7 eV reaching a local maximum at 4.6 ± 0.2 eV, this has been identified as the ${}^2B_1 \pi^*$ resonance described in Refs. [16, 17]. Further local maxima of the experimental TCS appear at 7, 8.5 and 10 eV, corresponding to two electronic excitation levels and ionisation, respectively. The 7.0 ± 0.2 eV inelastic feature is consistent with the position of the strongest optical band, with a maximum energy at 7.22 eV [26], which has been attributed to the excitation of the ${}^1B_2 + {}^1A_1$ states of pyridine. The 8.5 ± 0.2 eV structure is seen in Ref. [24], with a maximum energy value at 8.24 eV, and in the higher impact energy absorption measurements performed by Jonsson and Lindholm [27], being attributed to valence state excitations. Finally, the broad structure around 10 eV can be attributed to excited Rydberg states together with ionising transitions to continuum states. These electronic excitation and ionisation structures are not reproduced by the rotationally summed elastic scattering SMC calculation, and their lower result can reasonably be ascribed to these contributions in the measured TCS.

III. CONCLUDING REMARKS

Total electron scattering cross sections from pyridine have been measured in the energy range 1-200 eV by using a magnetically confined transmission-beam technique. Random uncertainty limits are less than 5%. Systematic errors arising from the scattering information missing within the detector's acceptance angle have been discussed and detailed information on the energy and angular resolution of the present measurements is detailed in order to allow a proper estimation of their magnitude. For energies above 10 eV present measurements show a

reasonable agreement, within the combined uncertainty limits, with our previous results [6], measured with a double spectrometer attenuation beam system. By subtracting the calculated magnitude of this systematic error from our theoretical IAM-SCAR+I+R total cross sections, we obtained a set of “corrected values” which have found to be in excellent agreement with our experimental data above 10 eV. Since the main contribution to this correction comes from the rotational excitation cross section we can conclude that our free rotating electric dipole representation based on the Born approximation to calculate dipole-induced rotational excitation cross sections reproduces the present experimental conditions well in the energy range 10-200 eV. This also indicates that interference effects affecting mainly the forward elastic scattering amplitudes [7], should be considered by independent atom calculations to properly agree with accurate integral cross section measurements. Below 10 eV we have found reasonable agreement with the SMC [4] calculation in terms of resonance positions corresponding to the trapping of an electron in two of the three π^* orbitals of pyridine at 1.2-1.6 and 4-5.5 eV, respectively. A feature at 3 eV has also been attributed to the ground state vibrational excitation cross sections, with a maximum contribution to the TCS of about $10 \times 10^{-20} \text{ m}^2$. The R-matrix calculation [5] seems to be less accurate in finding the position of the shape resonances. Other inelastic features have been identified as electronic excitation and ionisation transitions consistent with early electron spectroscopy studies [24, 26, 27]. These cross sections for pyridine facilitate further electron transport simulations in biologically relevant media.

ACKNOWLEDGEMENTS

This experimental study has partially been supported by the Spanish Ministry MINECO (Project FIS 2016-80440) and the FP7- European Union-ITN (Project 608163-ARGENT). A.I.L. also acknowledges the “Garantía Juvenil” grant programme from MINECO. J. J. acknowledges support from the Master’s Programme of the Universidad Complutense de Madrid.

-
- [1] *Radiation Damage in Biomolecular Systems*, G. García Gómez-Tejedor, and M. C. Fuss, Eds (Springer: London, 2012).
 - [2] I. Baccarelli, I. Bald, F. A. Gianturco, E. Illeberger, and J. Kopyra, *Phys. Rep.* **508**, 1 (2011).
 - [3] M. C. Fuss, L. Ellis-Gibblings, D. B. Jones, M. J. Brunger, F. Blanco, A. Muñoz, P. Limão-Vieira, and G. García, *J. Appl. Phys.* **117**, 214701 (2015).
 - [4] A. S. Barbosa, D. F. Pastega, and M. H. F. Bettega, *Phys. Rev. A* **88**, 022705 (2013).
 - [5] A. Sieradzka, F. Blanco, M. C. Fuss, Z. Mašín, J. D. Gorfinkiel, and G. García, *J. Phys. Chem. A* **118**, 6657 (2014).
 - [6] A. Traoré Dubuis, F. Costa, F. Ferreira da Silva, P. Limão-Vieira, J. C. Oller, F. Blanco, and G. García, *Chem. Phys. Lett.* **699**, 182 (2018).
 - [7] F. Blanco, L. Ellis-Gibblings, and G. García, *Chem. Phys. Lett.* **645**, 71 (2016).

- [8] A. Muñoz, J. C. Oller, F. Blanco, J. D. Gorfinkiel, P. Limao-Vieira and G. García, *Phys. Rev. A* **76**, 052707 (2007).
- [9] W. Tattersall, L. Chiari, J. R. Machacek, E. Anderson, R. D. White, M. J. Brunger, S. J. Buckman, G. Garcia, F. Blanco, and J. P. Sullivan, *J. Chem. Phys.* **140**, 044320 (2014).
- [10] *NIST Standard Reference Database Number 101*. Johnson, R. D., III, Ed. (2011). <http://cccbdb.nist.gov/>.
- [11] A. I. Lozano, J. C. Oller, K. Krupa, F. Ferreira da Silva, P. Limão-Vieira, F. Blanco, A. Muñoz, R. Colmenares, and G. García, *Rev. Sci. Instrum.* **89**, 063105 (2018).
- [12] Y. Itikawa *J. Phys. Chem. Ref. Data* **35**, 31 (2006).
- [13] C. Szymtkowski and K. Maciag, *Phys. Script.* **54**, 271 (1996)
- [14] F. Blanco and G. García, *Phys. Rev. A* **67**, 022701 (2003).
- [15] F. Blanco and G. García, *Phys. Lett. A* **317**, 458 (2003).
- [16] Z. Mašín and J. Gorfinkiel, *J. Chem. Phys.* **137**, 204312 (2012).
- [17] I. Nenner and G. J. Schultz, *J. Chem. Phys.* **62**, 1747 (1975).
- [18] A. Modeli and P. Burrow, *J. Electron Spectrosc. Relat. Phenom.* **32**, 263 (1983).
- [19] R. R. Lucchese and F. A. Gianturco, *Int. Rev. Phys. Chem.* **15**, 429 (1996).
- [20] A. G. Sanz, M. C. Fuss, F. Blanco, F. Sebastianelli, F. A. Gianturco, and G. García, *J. Chem. Phys.* **137**, 124103 (2012).
- [21] A. Jain, *J. Phys. B.* **21**, 905 (1988).
- [22] A. S. Dickinson, *J. Phys. B.* **10**, 967 (1977).
- [23] NIST Web Book of Chemistry, <https://webbook.nist.gov/chemistry/>
- [24] I. C. Walker, M. H. Palmer, and A. Hopkirk, *Chem. Phys.* **141**, 365, (1989).
- [25] M. J. Brunger, K. Ratnavelu, S. J. Buckman, D. B. Jones, A. Muñoz, F. Blanco, and G. García, *Eur. Phys. J. D* **70**, 46 (2016).
- [26] A. Bolovinos, P. Tsekeris, J. Philis, E. Pantos, and G. Anditsopoulos, *J. Mol. Spectrosc.* **103**, 240 (1984).
- [27] B. O. Jonsson and E. Lindholm, *Int. J. Mass Spectrom. Ion Phys.* **3**, 385 (1969).



Contents lists available at ScienceDirect

Chemical Physics Letters

journal homepage: www.elsevier.com/locate/cpllett

Research paper

Total electron scattering cross section from sevoflurane by 1–300 eV energy electron impact

A.I. Lozano^{a,b}, F. Ferreira da Silva^c, F. Blanco^d, P. Limão-Vieira^c, G. García^{a,*}^a Instituto de Física Fundamental, Consejo Superior de Investigaciones Científicas (CSIC), Serrano 113-bis, 28006 Madrid, Spain^b Escuela de Doctorado de la UNED–Programa de Doctorado en Ciencias, 28015 Madrid, Spain^c Atomic and Molecular Collisions Laboratory, CEFITEC, Department of Physics, Universidade NOVA de Lisboa, 2829-516 Caparica, Portugal^d Departamento de Física Atómica, Molecular y Nuclear, Facultad de Ciencias Físicas, Universidad Complutense de Madrid, E-28040 Madrid, Spain

ARTICLE INFO

Article history:

Received 8 June 2018

In final form 2 July 2018

Available online 3 July 2018

ABSTRACT

We report on novel total electron scattering cross section (TCS) measurements for electrons scattering from sevoflurane, at incident electron impact energies in the range 1–300 eV. The experimental results, obtained from a newly implemented magnetic beam apparatus based in Madrid, are compared with theoretical results from the independent atom model with screening corrected additivity rule including interference effects and rotational excitation (IAM-SCAR+R). A very good level of agreement has been found between the present experimental and theoretical data at above about 20 eV electron impact and to within the experimental uncertainties.

© 2018 Elsevier B.V. All rights reserved.

1. Introduction

Since the first use of ether as a general anaesthetic in 1842 by Crawford Williamson Long, inhaled anaesthetics have been widely used in surgical practice. The international community has been focused in understanding the role of such chemical compounds within the physiological environment, however how a given drug reversibly alters the central nervous system function still remains poorly understood. Currently, it is known that inhaled anaesthetics can modify the activity of a wide variety of proteins [1–4] by binding to discrete sites. Such knowledge has changed the traditional notion that all general anaesthetics act non-specifically. Thus, focusing on a knowledge of the molecular structure and chemical properties of these molecules may further help our understanding of their molecular reactivity and thereby ultimately improve the clinical utility of general anaesthetics. In this study we have focused on the important halogenated inhaled anaesthetic, sevoflurane (Fig. 1), which was introduced into clinical practice in the 1990s. Nowadays, it is one of the most used for induction and maintenance of general anaesthesia in different types of surgery and is also commonly used in children's clinical practice as well as in veterinary use. Sevoflurane possesses properties that are well attuned to an inhalation anaesthetic agent, due to its low solubility in blood in comparison with other inhaled anaesthetics like halothane and isoflurane [5].

An *ab initio* study, using both restricted Hartree-Fock (RHF) and hybrid B3LYP DFT quantum chemistry methods, to investigate the structure, charge distribution and electric dipole moment of sevoflurane (C₄H₃F₇O) has been performed by Tang et al. [6]. These authors reported that even within the same –CF₃ group, the RHF and DFT bond lengths and angles are not kept identical due to the overall molecular asymmetry which also causes a complex charge distribution. The structure of the anaesthetic haloether sevoflurane has been determined using Fourier-transform microwave spectroscopy, where complementary Stark effect measurements obtained its electric dipole moment to be 2.27D [7]. Vibrational assignments have been reported by Dom et al. [8] in infrared spectroscopy experiments together with several sevoflurane/benzene complexes. These complexes have interactions which are interesting from the chemical and biological points of view, since they may serve to model local interactions of protein receptors with aromatic side-chain molecules [9]. Langbein et al. [10] reported on volatile anaesthetics and their relevance to atmosphere chemistry, together with the role of chlorofluorocarbons (CFC) and halons in damaging the stratospheric ozone layer. Finally, we have recently explored by means of experimental and theoretical methods, the elastic differential and integral cross sections, for electrons scattering from sevoflurane in the 10–50 eV impact energy range [11].

In this paper, we include experimental data of total electron scattering cross sections from sevoflurane in the energy range 1–300 eV using a magnetically confined experimental system [12]. These experimental data are compared with results from

* Corresponding author.

E-mail address: g.garcia@csic.es (G. García).<https://doi.org/10.1016/j.cpllett.2018.07.005>

0009-2614/© 2018 Elsevier B.V. All rights reserved.

Total electron scattering cross section from sevoflurane by 1-300 eV energy electron impact

A. I. Lozano,^{1,2} F. Ferreira da Silva,³ F. Blanco,⁴ P. Limão-Vieira³ and G. García^{1*}

¹ Instituto de Física Fundamental, Consejo Superior de Investigaciones Científicas (CSIC), Serrano 113-bis, 28006 Madrid, Spain

² Escuela de Doctorado de la UNED-Programa de Doctorado en Ciencias, 28015 Madrid, Spain

³ Atomic and Molecular Collisions Laboratory, CEFITEC, Department of Physics, Universidade NOVA de Lisboa, 2829-516, Caparica, Portugal

⁴ Departamento de Física Atomica, Molecular y Nuclear, Facultad de Ciencias Fisicas, Universidad Complutense de Madrid, E-28040 Madrid, Spain

Abstract

We report on novel total electron scattering cross section (TCS) measurements for electrons scattering from sevoflurane, at incident electron impact energies in the range 1-300 eV. The experimental results, obtained from a newly implemented magnetic beam apparatus based in Madrid, are compared with theoretical results from the independent atom model with screening corrected additivity rule including interference effects and rotational excitation (IAM-SCAR+I+R). A very good level of agreement has been found between the present experimental and theoretical data at above about 20 eV electron impact and to within the experimental uncertainties.

* Corresponding author.

E-mail address: g.garcia@csic.es (G. García).

1. Introduction

Since the first use of ether as a general anaesthetic in 1842 by Crawford Williamson Long, inhaled anaesthetics have been widely used in surgical practice. The international community has been focused in understanding the role of such chemical compounds within the physiological environment, however how a given drug reversibly alters the central nervous system function still remains poorly understood. Currently, it is known that inhaled anaesthetics can modify the activity of a wide variety of proteins [1-4] by binding to discrete sites. Such knowledge has changed the traditional notion that all general anaesthetics act non-specifically. Thus, focusing on a knowledge of the molecular structure and chemical properties of these molecules may further help our understanding of their molecular reactivity and thereby ultimately improve the clinical utility of general anaesthetics. In this study we have focused on the important halogenated inhaled anaesthetic, sevoflurane (Fig. 1), which was introduced into clinical practice in the 1990s. Nowadays, it is one of the most used for induction and maintenance of general anaesthesia in different types of surgery and is also commonly used in children's clinical practice as well as in veterinary use. Sevoflurane possesses properties that are well attuned to an inhalation anaesthetic agent, due to its low solubility in blood in comparison with other inhaled anaesthetics like halothane and isoflurane [5].

An *ab initio* study, using both restricted Hartree-Fock (RHF) and hybrid B3LYP DFT quantum chemistry methods, to investigate the structure, charge distribution and electric dipole moment of sevoflurane ($C_4H_3F_7O$) has been performed by Tang *et al.* [6]. These authors reported that even within the same $-CF_3$ group, the RHF and DFT bond lengths and angles are not kept identical due to the overall molecular asymmetry which also causes a complex charge distribution. The structure of the anaesthetic haloether sevoflurane has been determined using Fourier-transform microwave spectroscopy, where complementary Stark effect measurements obtained its electric dipole moment to be 2.27D [7]. Vibrational assignments have been reported by Dom *et al.* [8] in infrared spectroscopy experiments together with several sevoflurane/benzene complexes. These complexes have interactions which are interesting from the chemical and biological points of view, since they may serve to model local interactions of protein receptors with aromatic side-chain molecules [9]. Langbein *et al.* [10] reported on volatile anaesthetics and their relevance to atmosphere chemistry, together with the role of chlorofluorocarbons (CFC) and halons in damaging the stratospheric ozone layer. Finally, we have recently explored by means of experimental and theoretical methods, the elastic

differential and integral cross sections, for electrons scattering from sevoflurane in the 10-50 eV impact energy range [11].

In this paper, we include experimental data of total electron scattering cross sections from sevoflurane in the energy range 1-300 eV using a magnetically confined experimental system [12]. Those experimental data are compared with results from our *ab initio* independent atom model-screening-corrected additivity rule with interference and rotational terms (IAM-SCAR+I+R) method [13-15]. Excellent agreement is found between them at energies above about 20 eV. The remainder of the present paper is structured as follows. In Sec. II, following this introduction, we provide a brief description of the experimental configuration and the theoretical methodology. In Sec. III we present and discuss our experimental and theoretical results. Finally, in Sec. IV, some conclusions from the present work are drawn.

2. Experimental and theoretical methods

A. Experimental setup

Figure 2 shows a schematic diagram of the experimental setup which has been developed and implemented at CSIC, Madrid, and which is intended to perform low energy electron scattering from molecular targets using a strong confining axial magnetic field. A thorough description of the main working principles and experimental details has been given recently [12, 16]. Briefly, it is based on the magnetic confinement of an electron beam that passes through a gas trap and a scattering chamber prior to its detection by an MCP. Such a strong magnetic field (~ 0.1 T) ensures that the electron's path is not affected by external fields (such as the earth's magnetic field), in particular at low kinetic energies. The electron kinetic energy (E) within a magnetic field can be separated into the parallel (\parallel) and perpendicular (\perp) components of the velocity, relative to the axial field direction (gyromotion). As described in Ref. [12] under these axial magnetic confinement conditions, any collision event in the gas trap/scattering chamber converts the expected scattering angle (θ) into a kinetic energy loss in the direction parallel to the beam (E_{\parallel}), according to $E_{\parallel} = E \cos^2 \theta$. As clearly denoted in figure 2, the system comprises five regions (1. electron gun, 2. gas trap, 3. pulse-controller, 4. scattering chamber, and 5. analyser-detector region) which are surrounded by solenoids that apply independent magnetic fields to each region. These regions, differentially pumped by means of three turbomolecular pumps, are connected by small orifices (1.5 mm) in order to create a well-defined region of constant pressure in both the gas trap and the scattering chamber. The

background pressure in the electron gun and analyser-detector regions is typically of the order of 10^{-8} Torr. In the pulse-controller region, the background pressure is higher (10^{-6} Torr) since the typical nitrogen (N_2) pressure inside the gas trap is 6×10^{-2} Torr. The electron beam, originating from the electron gun with a typical resolution $\Delta E = 500$ meV (FWHM) passes through the N_2 gas trap where electrons are forced to lose some of their initial kinetic energy, due to excitation of vibrational and discrete electronic states, to finally acquire a given set energy. In this process, the initial energy beam spread is also reduced [17] down to 160-350 meV, depending on the incident energy. Next, the beam emerging from the gas trap is pulsed with a typical time duration of 50 ms and a frequency of 10 Hz. The electron beam is then transported to the scattering chamber, where the target molecule (sevoflurane here) is admitted via a variable leak valve. Note that the pressure in the scattering chamber is measured by a Baratron capacitance manometer. After passing into the analyser-detector region, electrons are energy-selected by a retarding potential analyser (RPA). Only electrons with a parallel component of kinetic energy higher than the RPA potential energy barrier may reach the detector. The detection system is operated in a single-pulse counting mode and the MCP anode is positively biased with ~ 2 kV. The current pulses collected at the anode are converted into voltage pulses by means of a charge sensitive preamplifier. That output signal is subsequently amplified and converted into TTL signal through the use of a constant fraction discriminator. The resulting signals are finally transferred to the data acquisition system connected to a computer implemented with LabView software.

B. Beam energy calibration and data validation

Central to a valid measurement for the magnitude and shape of the total cross section, an accurate knowledge of the electron beam energy in the scattering chamber is needed. Such accurate information is also needed to benchmark the validity of the cross section measurements from the current setup. Thus, the present electron energy is calibrated using the well-known nitrogen resonance feature at ~ 2.5 eV [18, 19, 20] and our nitrogen total electron scattering cross section, in the energy range 1-20 eV, compares very favourably with the data from Szmytkowski *et al.* [18] to within 3% difference. Another important validation is to ensure that there are no significant changes in the absolute pressure value measured along the collision path length. In order to check that we have measured total cross sections (TCSs) from nitrogen, monitoring the gas pressure from two different manometers placed at both ends of the scattering chamber. No effect was observed.

C. Data acquisition methodology

The current data acquisition methodology includes the following protocols:

I. Sevoflurane was supplied by Sigma-Aldrich with a quoted purity of 99%, and we note that no further purification was undertaken by us. However, the sample was degassed by repeated freeze-pump-thaw cycles prior to use in order to minimise any impurities.

II. Before sample admission to the scattering chamber, the electron energy resolution was further improved by setting optimal magnetic fields in each section of the experimental apparatus followed by a reduction of ~75% of the transmitted intensity. In the latter case this was achieved by selecting a proper retarding potential value [12].

III. With the purpose of minimizing any possible multiple scattering effects, a convenient range of target gas pressures, during the attenuation measurements, was determined. In the present case we obtained the optimal pressure region from 0.5 to 6.0 mTorr. Note that for each energy, we have recorded at least three scans to achieve a statistical reproducibility $\leq 5\%$.

IV. The total electron scattering cross sections are then obtained for each energy by using the Beer-Lambert attenuation law:

$$I = I_0 e^{-nl\sigma_T} = I_0 e^{-pl\sigma_{exp}/kT} , \quad (1)$$

where I_0 is the intensity without attenuation, σ_{exp} is the experimental total scattering cross section, n is the density of the target gas, p is the partial pressure of the sample, l is the collision path length (40 mm), k is the Boltzmann constant, and T is the gas temperature (K). In Fig. 3 we plot the typical attenuation curves for $E = 1, 3, 13, 30, 70$ and 100 eV electron impact together with their exponential fit curves. Note that the excellent fit to the data, at each energy, confirms that multiple scattering effects were minimised in this study. The corresponding slopes provide directly the experimental total scattering cross section, σ_{exp} .

D. Experimental uncertainties

Systematic and random errors include contributions from the uncertainties in the collision path length, the sample gas pressure measurements, the attenuation curve fit function and the standard deviation from the different sets of measurements at the same energy (which comprise any filament and temperature instability during the measurements). Combining the aforementioned factors, a general experimental uncertainty in the range 1.0-4.7% is obtained. In addition, an inherent systematic error of the present experimental technique

is linked to the energy resolution which is related with the angular acceptance [12,15,16], entailing “missing angles” in the forward and backward scattering directions. The angular resolution ($\Delta\theta^\circ$) can be calculated from the energy resolution (ΔE) as:

$$\Delta\theta^\circ = \arcsin \sqrt{\frac{\Delta E}{E}} \quad . \quad (2)$$

The method used to obtain the energy resolution is reported in detail in refs. [12, 16]. In the present experiment the energy resolution and the detector angular acceptance are $\Delta E \leq 0.35$ eV and $\Delta\theta \leq 26.60^\circ$, although we note that optimum values of 0.16 eV and 2.0° have been obtained here (see Table I).

E. Theoretical method

In order to further our knowledge on the electron scattering process from sevoflurane, and help to interpret the experimental data, we have used the IAM-SCAR+I method (independent atom model (IAM) applying the screened additivity rule (SCAR) with interferences terms included (I)). This method has been described in detail in previous publications [13-16,21,22]. Briefly, the molecular target is described as an aggregate of its individual atoms (i.e. C, H, F and O in this case). Each atomic target is represented by an *ab initio* interacting complex optical potential given by:

$$V_{opt}(\vec{r}) = V_R(\vec{r}) + iV_{abs}(\vec{r}) \quad . \quad (3)$$

In Eq. (3), the real part accounts for elastic scattering while the imaginary part represents the inelastic processes which are considered as the ‘absorption part’ following the procedure of Staszewska *et al.* [23]. The real part is divided into three terms that include:

$$V_R(\vec{r}) = V_s(\vec{r}) + V_{ex}(\vec{r}) + V_{pol}(\vec{r}) \quad , \quad (4)$$

where V_s represents a static term derived from a Hartree-Fock calculation of the atomic charge distribution [24], V_{ex} an exchange term to account for the indistinguishability of the incident and target electrons [25] and V_{pol} a long-range polarization term [26].

The molecular cross sections are obtained from the atomic data by the screening corrected additivity rule (SCAR) procedure [27], incorporating interference (I) term corrections [14], by summing all the relevant atomic amplitudes, including the phase coefficients. In this approach we obtain the molecular differential scattering cross section (DCS), which integrated over all the scattered electron angular range gives the integral scattering cross section (ICS). Moreover, by taking the sum of the ICS for all open channels (elastic ICS and inelastic ICS) the TCS is obtained. Note that we do not include at this stage any

contribution from vibrational and rotational excitation processes. However, for polar molecules, as is the case of sevoflurane, with a permanent dipole moment of 2.27 D [7], the rotational driven cross section (dipole-excitation cross sections (+R)) is obtained [16] and added to the IAM-SCAR+I TCS [28].

3. Results and discussion

In table I we present the experimental total electron scattering cross section data from sevoflurane, as a function of the electron energy, together with the estimated uncertainties, and energy and angular resolutions. Note that in general our poorer angular resolutions correspond to our lower electron impact energies, even at better energy resolutions. To perform a valid comparison between the experimental data and the calculated TCSs, the angular acceptance is interpreted as corresponding to the so-called missing angles in the forward and backward directions, which results in relatively lower measured TCS values [29]. Hence, the DCSs obtained from the IAM-SCAR+I+R computations have to be integrated over the range $[\Delta\Theta^\circ, 180^\circ-\Delta\Theta^\circ]$ with those results being subtracted from the IAM-SCAR+I+R TCS to enable a more valid comparison to our measured results. The tabulated TCS values from this procedure are given in table II, and we denote them as our IAM-SCAR+I+R- $\Delta\Theta$ TCS.

Figure 4 depicts the present experimental results on the total cross section together with our *ab initio* calculated TCS with (IAM-SCAR+I+R) and without (IAM-SCAR+I) rotational contributions as well as those accounting for the missing angles, i.e. our (IAM-SCAR+I+R- $\Delta\Theta$) TCS. The uncertainty limits of both our experimental, and calculated IAM-SCAR+I+R- $\Delta\Theta$ TCS data have also been included in this figure.

At this point of the discussion it is worth noting that the associated uncertainties from the IAM-SCAR+I+R- $\Delta\Theta$ TCS calculation are to within 10%, which is reasonable for electron impact energies > 20 eV (our typical calculation validity range), since at lower energies (< 20 eV), inherent limitations of the theoretical method may affect the results. The 10% uncertainty limit assigned to our calculation for energies above 20 eV is supported by comparisons with accurate experimental data from similar molecules (see Ref. [15] and references therein). Another interesting aspect is the good agreement between the experimental data and the IAM-SCAR+I+R- $\Delta\Theta$ TCS for electron energies > 40 eV, where a $< 13\%$ difference is observed. However, for lower electron impact energies (< 40 eV), this discrepancy increases ($> 14\%$), being particularly significant for $E < 4$ eV. Nonetheless, it is fair to say that both these sets of results agree reasonably well to within

the combined uncertainty limits for electron impact energies above about 20 eV. The importance of considering the angular acceptance, when comparing the IAM-SCAR+I+R and the IAM-SCAR+I+R- $\Delta\Theta$ TCS results (see Fig. 4), is in support of the procedure established to account for the missing angles contribution. In addition, a closer inspection of Fig. 4 reveals

some weak features visible between 5 and 10 eV and a broad hump centered within 30-50 eV – which is the typical structure for fluorine rich targets [30]. Since there is currently no other available data in the literature to compare against for electron scattering from sevoflurane, this latter observation remains speculative.

V. Conclusions

The present work provides for the first time total electron scattering cross section data from sevoflurane at incident energies in the range 1-300 eV, using a recently developed and implemented experimental setup [12] that makes use of a strong axial magnetic field. The excellent agreement between the measured total cross sections and the *ab initio* calculations (typically above 20 eV), considering both the angular limitation in the measurements and the validity range of the calculations, suggests that the present results form a good basis for assembling a cross section data base for modelling studies on electron interactions with sevoflurane [31]. Certainly, the work foreshadowed in Lange *et al.* [11] will further add to that cross section data base, providing crucial further information for understanding its chemical and biological activity, for this important molecule.

Acknowledgments

Authors acknowledge partial financial support from the Spanish Ministerio de Economía y Competitividad (Project No. FIS2016-80440). F.F.S. also acknowledges the Portuguese National Funding Agency FCT through Researcher Contract No. IF-FCT IF/00380/2014, and, together with P.L.V., the Research Grant No. UID/FIS/00068/2013. Authors also acknowledge Prof. M. J. Brunger and Dr. L. Campbell their valuable help in discussing results and editing procedures.

References

- [1] R. G. Eckenhoff and J. S. Johansson, *Pharmacol. Rev.* 49, 343–367, 1997
- [2] R. Pidikiti, T. Zhang, K. M. G. Mallela, M. Shamim, K. S. Reddy, and J. S. Johansson, *Int. Congr. Ser.* 1283, 155–159, 2005
- [3] P. Tang, V. Simplaceanu, and Y. Xu, *Biophys. J.* 76, 2346–2350, 1999
- [4] P. Tang, R. G. Eckenhoff, and Y. Xu, *Biophys. J.* 78, 1804–1809, 2000
- [5] R. M. Jones, *Br. J. Anaesth.* 65, 527–536, 1990
- [6] P. E. I. Tang, I. Zubryzcki, and Y. A. N. Xu, *J. Comput. Chem.* 22, 436–444, 2001.
- [7] A. Lesarri, A. Vega-Toribio, R. D. Suenram, D. J. Brugh, and J.-U. Grabow, *Phys. Chem. Chem. Phys.* 12, 9624, 2010
- [8] J. J. J. Dom *et al.*, *Phys. Chem. Chem. Phys.* 13, 14142, 2011
- [9] T. X. Cui, V. Bondarenko, D. J. Ma, C. Canlas, N. R. Brandon, J. S. Johansson, Y. Xu and P. Tang, *Biophys. J.* 94, 4464–4472, 2008
- [10] T. Langbein, H. Sonntag, D. Trapp, A. Hoffmann, W. Malms, E.-P. Röth, V. Mörs, and R. Zellner, *Br. J. Anaesth.* 82, 66–73, 1999
- [11] E. Lange, A. M. Lozano, F. Blanco, M. H. F. Bettega, G. García, P. Limão-Vieira, and F. Ferreira da Silva, in preparation, 2018
- [12] A. I. Lozano, J. C. Oller, K. Krupa, P. Limão-Vieira, F. Blanco, A. Muñoz, R. Colmenares, and G. García, *Rev. Sci. Instrum.*, in press, 2018
- [13] F. Blanco, J. Rosada, A. Illana, and G. García, *Phys. Lett. A* 374, 4420, 2010
- [14] F. Blanco, L. Ellis-Gibbings, and G. García, *Chem. Phys. Lett.* 645, 71, 2016
- [15] A. Traore Dubuis, A. Verkhovtsev, L. Ellis-Gibbings, K. Krupa, F. Blanco, D. B. Jones, M. J. Brunger, and G. García, *J. Chem. Phys.* 147, 054301, 2017
- [16] M. C. Fuss, A. G. Sanz, F. Blanco, J. C. Oller, P. Limão-Vieira, M. J. Brunger, and G. García, *Phys. Rev. A* 88, 042702, 2013
- [17] J. P. Sullivan, S. J. Gilbert, J. P. Marler, R. G. Greaves, S. J. Buckman, and C. M. Surko, *Phys. Rev. A* 66, 042708, 2002
- [18] C. Szmytkowski, K. Maciag, and G. Karwasz, *Phys. Scripta* 54, 271–280, 1996
- [19] M. J. Brunger and S. J. Buckman, *Phys. Repts.* 357, 215–458, 2002
- [20] K. R. Hoffmann *et al.*, *Phys. Rev. A* 25, 1393–1403, 1982
- [21] A. I. Lozano, J. C. Oller, D. B. Jones, R. F. da Costa, M. T. do N. Varella, M. H. F. Bettega, F. Ferreira da Silva, P. Limão-Vieira, M. A. P. Lima, R. D. White, M. J. Brunger, F. Blanco, A. Muñoz, and G. García, *Phys. Chem. Chem. Phys.*, submitted, 2018
- [22] D. B. Jones, F. Blanco, G. García, R. F. da Costa, F. Kossoski, M. T. do N. Varella, M. H. F. Bettega, M. A. P. Lima, R. D. White, and M. J. Brunger, *J. Chem. Phys.* 147, 244304, 2017
- [23] G. Staszewska, D. W. Schwenke, D. Thirumalai, and D. G. Truhlar, *Phys. Rev. A* 28, 2740, 1983
- [24] R. D. Cowan, *The Theory of Atomic Structure and Spectra* (University of California Press, London, 1981)
- [25] M. E. Riley and D. G. Truhlar, *J. Chem. Phys.* 63, 2182, 1975
- [26] X. Zhang, J. Sun, and Y. Liu, *J. Phys. B: At. Mol. Opt. Phys.* 25, 1893, 1992
- [27] F. Blanco and G. García, *Phys. Lett. A* 330, 230, 2004
- [28] A. Zecca, L. Chiari, G. García, F. Blanco, E. Trainotti, and M. J. Brunger, *J. Phys. B* 43, 215204, 2010
- [29] M. J. Brunger, S. J. Buckman, and K. Ratnavelu, *J. Phys. Chem. Ref. Data* 46, 023102, 2017
- [30] C. Szmytkowski, A. Domaracka, P. Mozejko, E. Ptasińska-Denga and S. Kwitniewski, *J. Phys. B* 38, 745, 2005.
- [31] M. J. Brunger, *Int. Rev. Phys. Chem.* 36, 333–376, 2017

Figure captions

Fig. 1. A schematic representation of the molecular structure of sevoflurane (colour online). Figure drawn using the Jmol software.

Fig. 2. Schematic diagram of the present experimental configuration: (1) electron gun, (2) gas trap, (3) pulse-controller, (4) scattering chamber, (5) analyser-detector, (6) nitrogen inlet, (7) gas target inlet, (8) cooling water inlet/outlet, (9) water jacket, (10) scattering cell and scattering chamber focusing electrodes, (11) various transmission grids, (P_1 , P_2 , P_3) turbomolecular pumps, (RPA) retarding potential analyser, (MCP) dual micro-channel-plate assembly, (B_{eg} , B_{GT} , B_P , B_{SC} , B_{AD}) magnetic fields in the electron gun, gas trap, pulse-controller/interface chamber, scattering chamber and detector area, respectively. Note that this figure is not drawn to scale (colour online).

Fig. 3. Representative attenuation curves with their corresponding exponential fit functions (colour online). See also legend on figure.

Fig. 4. Experimental total electron scattering cross sections from sevoflurane compared with our ab initio TCS calculations with (IAM-SCAR+I+R) and without (IAM-SCAR+I) rotations. The square points represent the integrated values from our IAM-SCAR+I+R calculation, over the range $[\Delta\theta^\circ, 180^\circ-\Delta\theta^\circ]$ (colour online), that accounts for the missing angles in the measured data. See also legend in figure and text.

Table captions

Table I. Experimental total electron scattering cross section data and error estimates from sevoflurane. Also shown are the relevant energy resolutions and “missing angle” ranges for each incident electron energy.

Table II. Total cross sections obtained from our IAM-SCAR+I+R calculations, but corrected for the missing angles over the angular range $[\Delta\theta^\circ, 180^\circ-\Delta\theta^\circ]$ in order to better correspond to our measured data.

Fig. 1. A schematic representation of the molecular structure of sevoflurane (colour online). Figure drawn using the Jmol software.

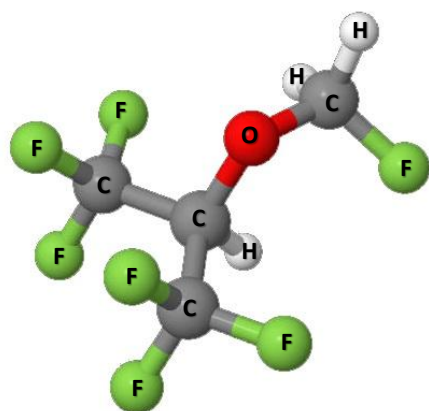


Fig. 2. Schematic diagram of the present experimental configuration: (1) electron gun, (2) gas trap, (3) pulse-controller, (4) scattering chamber, (5) analyser-detector, (6) nitrogen inlet, (7) gas target inlet, (8) cooling water inlet/outlet, (9) water jacket, (10) scattering cell and scattering chamber focusing electrodes, (11) various transmission grids, (P_1 , P_2 , P_3) turbomolecular pumps, (RPA) retarding potential analyser, (MCP) dual micro-channel-plate assembly, (B_{eg} , B_{GT} , B_P , B_{SC} , B_{AD}) magnetic fields in the electron gun, gas trap, pulse-controller/interface chamber, scattering chamber and detector area, respectively. Note that this figure is not drawn to scale (colour online).

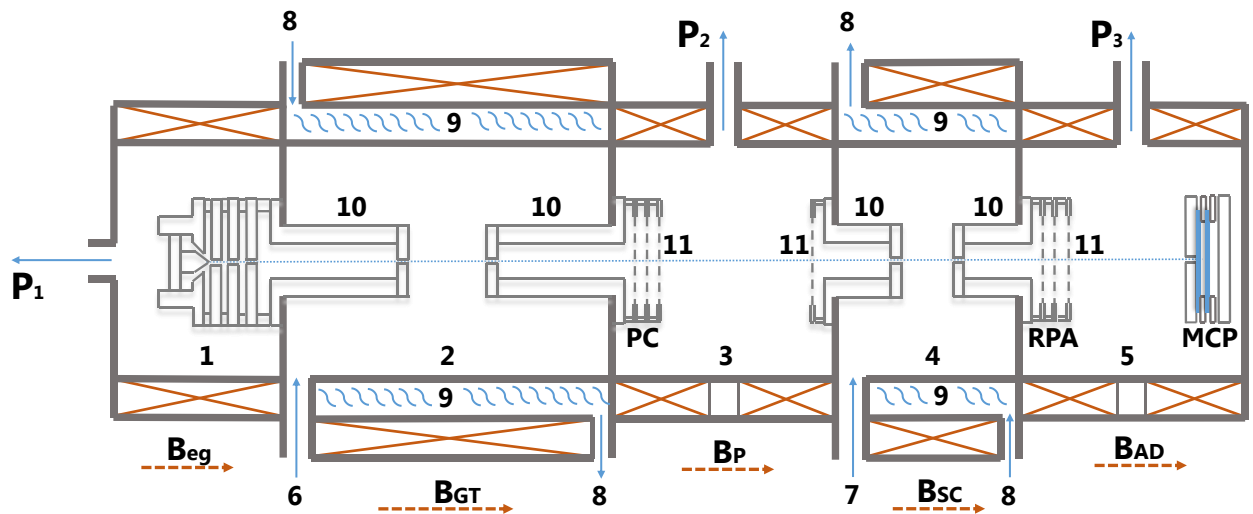


Fig. 3. Representative attenuation curves with their corresponding exponential fit functions (colour online). See also legend on figure.

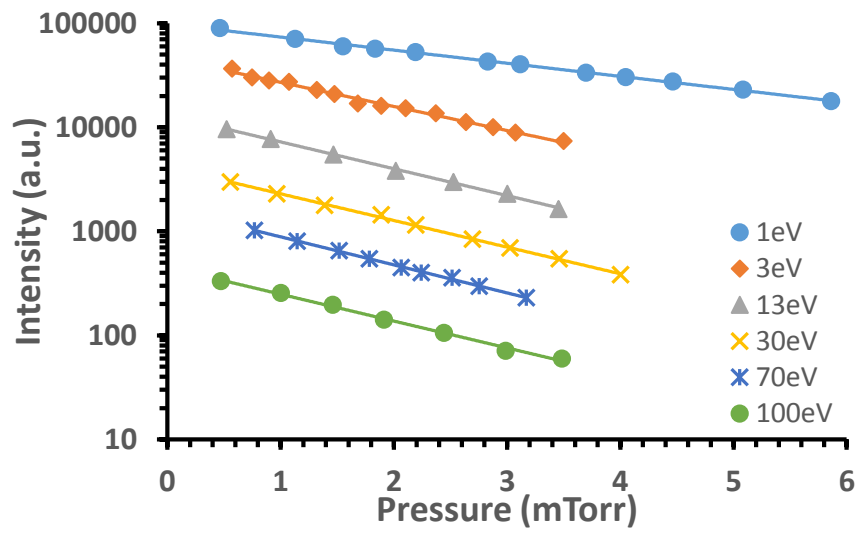


Fig. 4. Experimental total electron scattering cross sections from sevoflurane compared with our ab initio TCS calculations with (IAM-SCAR+I+R) and without (IAM-SCAR+I) rotations. The square points represent the integrated values from our IAM-SCAR+I+R calculation, over the range $[\Delta\theta^\circ, 180^\circ-\Delta\theta^\circ]$ (colour online), that accounts for the missing angles in the measured data. See also legend in figure and text.

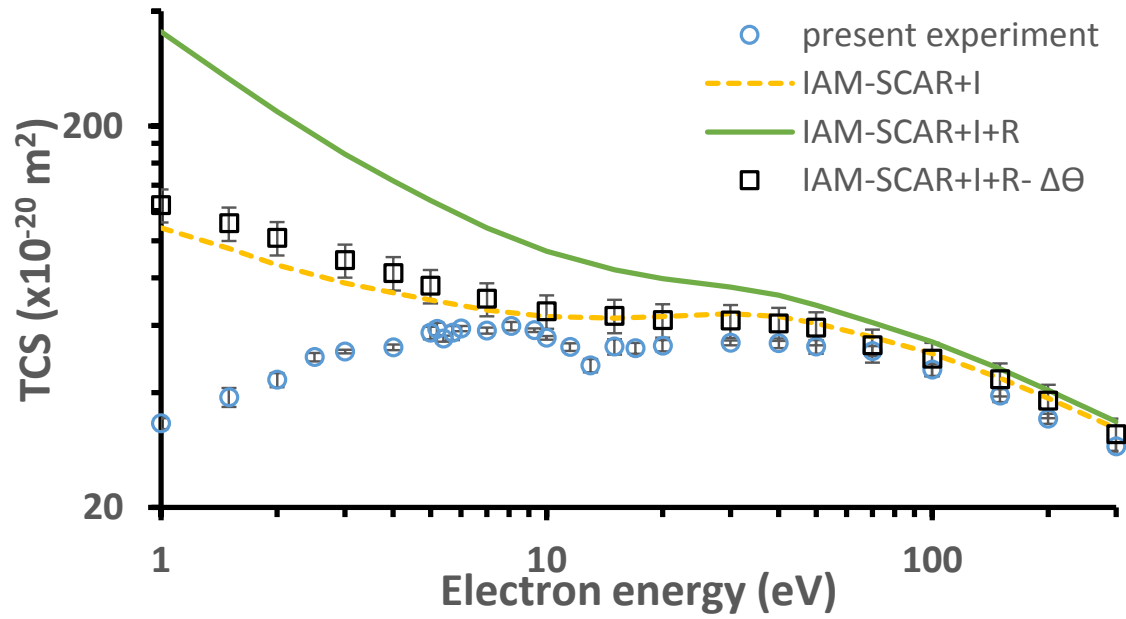


Table I. Experimental total electron scattering cross section data and error estimates from sevoflurane. Also shown are the relevant energy resolutions and “missing angle” ranges for each incident electron energy.

Energy (eV)	$\sigma_{\text{exp}} (10^{-20} \text{ m}^2)$	Statistical uncertainty (%)	Absolute total uncertainty limit (\pm)	ΔE (eV)	$\Delta\Theta$ (deg)
1.0	33.2	3.2	1.1	0.20	26.6
1.5	39.1	3.1	1.2	0.19	20.8
2.0	43.2	4.3	1.8	0.18	17.4
2.5	49.55	2.5	1.2	0.16	14.7
3.0	51.24	1.0	0.5	0.18	14.2
4.0	52.6	1.7	0.9	0.17	11.9
5.0	57.4	3.8	2.2	0.22	12.1
5.2	58.78	3.8	2.2	0.24	12.4
5.4	55.4	1.8	1.0	0.23	11.9
5.7	57.4	4.3	2.5	0.21	11.1
6.0	58.9	1.7	1.0	0.19	10.3
7.0	58.2	1.8	1.1	0.22	10.2
8.1	59.8	2.5	1.5	0.23	9.7
9.3	58.3	1.1	0.7	0.25	9.4
10	55.7	1.1	0.6	0.23	8.7
11.5	52.7	2.3	1.2	0.26	8.6
13	47.1	4.0	1.9	0.25	8.0
15	52.8	4.7	2.5	0.24	7.3
17	52.3	3.2	1.7	0.24	6.8
20	53.1	3.4	1.8	0.30	7.0
30	54.0	1.5	0.8	0.30	5.7
40	53.9	3.0	1.6	0.31	5.1
50	52.8	4.1	2.2	0.29	4.4
70	51.4	3.1	1.6	0.30	3.8
100	45.9	3.8	1.8	0.23	2.7
150	39.3	3.9	1.6	0.25	2.3
200	34.2	3.1	1.1	0.35	2.4
300	28.9	2.6	0.8	0.35	2.0

Table II. Total cross sections obtained from our IAM-SCAR+I+R calculations, but corrected for the ionising angles over the angular range $[\Delta\theta^\circ, 180^\circ-\Delta\theta^\circ]$ in order to better correspond to our measured data.

Energy (eV)	IAM-SCAR+I+R- $\Delta\theta$ TCS (10^{-20} m^2)
1.0	124.1
1.5	111.1
2.0	101.7
3.0	89.0
4.0	82.3
5.0	76.2
7.0	70.4
10	65.4
15	63.6
20	62.0
30	61.7
40	60.7
50	59.1
70	53.2
100	49.1
150	43.4
200	38.1
300	31.1



Total electron scattering cross sections from thiophene for the (1-300 eV) impact energy range

A. I. Lozano,^{1,2,a)} A. Loupas,^{3,4} F. Blanco,⁵ J. D. Gorfinkiel,⁴ and G. García^{1,6,b)}

¹Instituto de Física Fundamental, Consejo Superior de Investigaciones Científicas, Serrano 113-Bis, 28006 Madrid, Spain

²Escuela de Doctorado de la UNED-Programa de Doctorado en Ciencias, 28015 Madrid, Spain

³Laboratório de Colisões Atômicas e Moleculares, CEFITEC, Departamento de Física, Faculdade de Ciências e Tecnologia, Universidade Nova de Lisboa, Campus de Caparica, 2829-516 Lisbon, Portugal

⁴School of Physical Sciences, The Open University, Walton Hall, Milton Keynes MK7 6AA, United Kingdom

⁵Departamento de Física Atómica, Molecular y Nuclear, Universidad Complutense de Madrid, 28040 Madrid, Spain

⁶Centre for Medical Radiation Physics, University of Wollongong, Wollongong, NSW, Australia

(Received 30 July 2018; accepted 17 September 2018; published online 2 October 2018)

Experimental electron scattering cross sections for thiophene in the impact energy range from 1 to 300 eV have been measured with a magnetically confined electron transmission-beam apparatus. Random uncertainty limits have been estimated to be less than 5%, and systematic errors derived from acceptance angle limitations have also been identified and evaluated. Experimental values are compared with our previous low energy (1-15 eV) R-matrix and intermediate/high energy (15-300 eV) IAM-SCAR+I calculations finding reasonable agreement, within the combined uncertainty limits. Some of the low energy shape and core-excited resonances predicted by previous calculations are experimentally confirmed in this study. *Published by AIP Publishing.* <https://doi.org/10.1063/1.5050349>

I. INTRODUCTION

Electron interactions with complex molecules have been the subject of great interest in the last few years due to their relevance in important applications such as radiation damage^{1,2} and electron transport in plasmas³ and condensed media.⁴ These applications require evaluated differential (DCS) and integral (ICS) cross section data over a broad energy range for which different theoretical and experimental techniques need to be applied and the consistency between the corresponding results needs to be verified. In the case of thiophene (C₄H₄S), commonly used as an anti-inflammatory drug, we have recently calculated⁵ differential and integral elastic, integral inelastic and total electron cross sections over a broad energy range (0.1–1000 eV) by combining the R-matrix procedure for the lower energies with the IAM-SCAR+I method for intermediate and high energies. Our previous theoretical results were compared with experimental and theoretical data available in the literature (see Ref. 5 and references therein). In particular, the lower energy data were found to be in agreement with previous Schwinger multichannel with pseudopotentials (SMCPP) calculations,⁶ and the consistency with the IAM-SCAR+I higher energy results was found to be reasonably good. This provided a consistent picture of the scattering process in the whole energy range. However, an experimental validation of these cross section data is needed in order to ensure that they are appropriate for use in modelling and to establish some realistic uncertainty limits.

In this context, we present here absolute values for the total electron scattering cross section (TCS) from thiophene for impact energies ranging from 1 to 300 eV measured with a state-of-the-art magnetically confined electron transmission-beam apparatus⁷ together with a detailed analysis of their associated random and systematic uncertainty sources. Since the TCS corresponds to the sum of the ICS related to all the open channels at a given energy, they are excellent reference values to carry out the aforementioned validation.

The remainder of this paper is structured as follows: In Sec. II, some details on the experimental setup and procedure are given. A brief description of the calculation procedures which are relevant to this study are summarised in Sec. III. The current experimental results are presented and discussed in Sec. IV and compared with the available theoretical data. Our conclusions are finally summarized in Sec. V.

II. EXPERIMENTAL SETUP AND PROCEDURE

The experimental apparatus and techniques used for the present transmission-beam attenuation study have recently been described⁷ and so will not be detailed again here. In brief, a linear electron beam is confined by an intense (typically 0.1 T) axial magnetic field which converts any scattering event into a kinetic energy loss in the forward direction, i.e., parallel to the magnetic field (see Ref. 7 for full details). The primary electron beam, generated by an emitting filament, is cooled and confined in a magnetic nitrogen gas trap (GT) which reduces the initial energy spread of 500 meV down to about 100–200 meV. Pulsed voltages applied to the trap

^{a)}anita_ilm@iff.csic.es

^{b)}g.garcia@csic.es

Total electron scattering cross sections from thiophene for the (1-300 eV) impact energy range

A. I. Lozano,^{1,2, a} A. Loupas,^{3,5} F. Blanco,⁴ J. D. Gorfinkiel⁵ and G. García^{1, 6, b}

¹*Instituto de Física Fundamental, Consejo Superior de Investigaciones Científicas, Serrano 113-bis, 28006 Madrid, Spain*

²*Escuela de Doctorado de la UNED-Programa de Doctorado en Ciencias, 28015 Madrid, Spain*

³*Laboratório de Colisões Atómicas e Moleculares, CEFITEC, Departamento de Física, Faculdade de Ciências e Tecnologia, Universidade Nova de Lisboa, Campus de Caparica, 2829-516, Portugal*

⁴*Departamento de Física Atómica, Molecular y Nuclear, Universidad Complutense de Madrid, 28040 Madrid, Spain*

⁵*School of Physical Sciences, The Open University, Walton Hall, Milton Keynes, MK7 6AA, United Kingdom.*

⁶*Centre for Medical Radiation Physics, University of Wollongong, NSW, Australia*

Experimental electron scattering cross sections for thiophene in the impact energy range from 1 to 300 eV have been measured with a magnetically confined electron transmission-beam apparatus. Random uncertainty limits have been estimated to be less than 5 % and systematic errors derived from acceptance angle limitations have also been identified and evaluated. Experimental values are compared with our previous low energy (1-15 eV) R-matrix and intermediate/high energy (15-300 eV) IAM-SCAR+I calculations finding reasonable agreement, within the combined uncertainty limits. Some of the low energy shape and core-excited resonances predicted by previous calculations are experimentally confirmed in this study.

I. INTRODUCTION

Electron interactions with complex molecules have been the subject of great interest in the last few years due to their relevance in important applications such as radiation damage^{1,2} and electron transport in plasmas³ and condensed media.⁴ These applications require evaluated differential and integral cross section data over a broad energy range for which different theoretical and experimental techniques need to be applied and consistency between the corresponding results needs to be verified. In the case of thiophene (C₄H₄S), commonly used as anti-inflammatory drug, we have recently calculated⁵ differential and integral elastic, integral inelastic and total electron cross sections over a broad energy range (0.1-1000 eV) by combining the R-matrix procedure for the lower energies with the IAM-SCAR+I method for intermediate and high energies. Our previous theoretical results were compared with experimental and theoretical data available in the literature (see ref. 5 and references therein). In particular, the lower energy data were found to be in agreement with previous Schwinger multichannel with pseudopotentials (SMCPP) calculations⁶ and the consistency with the IAM-SCAR+I higher energy results was found to be reasonably good. This provided a consistent picture of the scattering process in the whole energy range. However, an experimental

^a anita_ilm@iff.csic.es

^b g.garcia@csic.es

validation of this cross section data is needed in order to ensure they are appropriate for use in modelling and to establish some realistic uncertainty limits.

In this context, we present here absolute values for the total electron scattering cross section (TCS) from thiophene for impact energies ranging from 1 to 300 eV measured with a state-of-the-art magnetically confined electron transmission-beam apparatus⁷ together with a detailed analysis of their associated random and systematic uncertainty sources. Since the TCS corresponds to the sum of the integral cross section (ICS) related to all the open channels at a given energy, they are excellent reference values to carry out the aforementioned validation.

The remainder of this paper is structured as follows. In Section II some details on the experimental setup and procedure are given. A brief description of the calculation procedures which are relevant to this study are summarised in section III. The current experimental results are presented and discussed in Section IV and compared with available theoretical data. Our conclusions are finally summarized in Section V.

II. EXPERIMENTAL SETUP AND PROCEDURE

The experimental apparatus and techniques used for the present transmission-beam attenuation study have recently been described⁷ and so will not be detailed again here. Briefly, a linear electron beam is confined by an intense (typically 0.1 T) axial magnetic field which converts any scattering event into a kinetic energy loss in the forward direction, i.e. parallel to the magnetic field (see Ref. 7 for full details). The primary electron beam, generated by an emitting filament, is cooled and confined in a magnetic nitrogen gas trap (GT) which reduces the initial energy spread of 500 meV down to about 100-200 meV. Pulsed voltages applied to the trap electrodes produce a pulsed electron beam with well-defined energy and narrow energy spread to enter the scattering cell. The scattering chamber (SC) is a 40 mm long gas cell, defined by two 1.5 mm diameter apertures, through which the pulsed electron beam passes when the thiophene pressure inside the chamber is varied from 0 to 5 mTorr (as measured by a MKS-Baratron 627B absolute capacitance manometer). Electrons emerging from the SC are analysed in energy by a retarding potential analyser (RPA) and finally detected by a double microchannel plate (MCP) electron multiplier operating in single counting mode. The total cross section (σ_T) is determined from the transmitted intensity, which follows the well-known Lambert-Beer attenuation law for ideal gases:

$$\ln\left(\frac{I}{I_0}\right) = -L\sigma_T n = -\frac{L\sigma_T}{kT} p, \quad (1)$$

where I is the transmitted electron intensity, I_0 the initial intensity, n the molecular gas density, L is the interaction region length, k is the Boltzmann constant, T is the absolute temperature and p is the gas pressure. T is derived from $T = \sqrt{T_c T_m}$, where T_c and T_m are the temperature of the scattering chamber measured with a thermocouple and the temperature of the Baratron gauge, respectively. Measurement conditions, data acquisition and data analysis are controlled by a custom designed LabView (National Instrument) programme.

For each incident electron energy, attenuation measurements were repeated at least 5 times in order to ensure that statistical uncertainties remained below 4%. Other random

uncertainties are related to the temperature measurement (within 1%, according to manufacturer's data) and the numerical fitting procedure (about 1%). By combining these uncertainties, a total uncertainty limit of 5 % has been determined for the present measurements. Systematic errors linked to the experimental technique are those connected to the so-called "missing angles".⁷ Due to the magnetic field confinement, the energy resolution determines the acceptance angle of the detector. As detailed in Ref. 7, and also in Fuss et al.⁸ and Sanz et al.⁹, the magnitude of this systematic error can be evaluated from our theoretical data by integrating the calculated differential elastic and rotational excitation cross sections over the "missing" experimental angles. This effect is especially important for polar molecules, as it is the case of thiophene ($\mu=0.52$ Debye¹⁰). The significance of this error source in the present experimental results will be discussed in Section IV.

Prior to making the present thiophene total cross section measurements, the performance of the new apparatus and our measurement techniques were thoroughly benchmarked against the known TCS values of N₂^{11,12} over the energy range of interest. Excellent agreement between our measured TCS data and the established values was found, giving us confidence in the validity of the TCS we have subsequently measured for thiophene.

III. THEORETICAL METHODS

As already mentioned, in order to cover the broad incident energy range considered in this study we have used two different theoretical methods of proven reliability in their respective energy ranges of applicability. For the lower energies (1-15 eV) we have applied the R-matrix method^{13,14} within the fixed-nuclei approximation using the UKRmol suite.¹⁵ As usual, in order to include the contribution of the higher order partial waves and properly account for the dipole interaction, a Born approximation based method, implemented in the program POLYDCS,¹⁶ has been used to determine the differential and integral cross sections. The general features of these methods and the particular details on their application to thiophene have been published elsewhere.⁵ We note only that the approach used by POLYDCS introduces the rotational motion into the scattering and that therefore, the Born-corrected 'elastic' cross section corresponds, in practice, to an electronically elastic but that includes rotational transitions from the rotational ground state ($J=0$) to rotational states with $0 \leq J \leq 9$.

As discussed in Ref. 5, physical considerations lead us to recommend the Born-corrected close coupling (CC) results (that we'll label R-matrix-CC-Born) as the most accurate of our R-matrix data. For intermediate and high energies (15-300 eV) we have used the latter version of our IAM-SCAR+I¹⁷ method together with an independent calculation based on the Born approximation (IAM-SCAR+I+R) to estimate the averaged dipole rotational excitation cross sections.¹⁸ Here we simply mention that including interference effects into the IAM-SCAR representation results in a clear increase in size of the differential elastic cross section for the smaller scattering angles,¹⁷ which consequently leads to an increase in the corresponding integral elastic cross sections. We have recently shown that for some benzene-like based molecules, such as pyridine, this increment can be of the order of 25-30% for the higher energies.¹⁹ The IAM-SCAR procedure has provided reasonable agreement for a wide variety of molecular targets for energies above ~ 20 eV,²⁰ but the role of the new interference terms still needs some further experimental validation. Inelastic scattering processes are not affected by the inclusion of the interference terms and a single cross section for all inelastic processes is

calculated from the imaginary part (absorption) of the interaction potential. However, as described in a recent article,²¹ by alternately using as the threshold energy of the absorption potential either the minimum electronic-state excitation energy or the ionisation energy we are able to extract the integral excitation and the integral ionisation cross sections from the calculated integral inelastic cross sections. We have recently shown that the total ionisation cross sections of some organic molecules,^{22,23} as derived from this procedure, are in fairly good agreement with the available experimental results.

IV. RESULTS AND DISCUSSION

The total electron scattering cross sections, in SI units, measured with the experimental set-up described above are shown in Table 1 together with our recent calculations using both the R-matrix-CC-Born and IAM-SCAR+I+R procedures mentioned in the previous sections.

Table 1. Present experimental electron scattering cross sections, TCS, their random uncertainty limits, the energy resolution (ΔE) and the acceptance angle of the detector ($\Delta\theta$) together with our R-matrix-CC-Born and IAM-SCAR+I+R calculations⁵. $\sigma(\Delta\theta)$ is the systematic error due to the acceptance angles as estimated with these calculations.

Energy (eV)	Experiment					Theory	
	TCS ($\times 10^{-20} \text{ m}^2$)	Random uncertainty ($\times 10^{-20} \text{ m}^2$)	ΔE (eV)	$\Delta\theta$ (deg)	$\sigma(\Delta\theta)$ ($\times 10^{-20} \text{ m}^2$)	R-matrix (CC-Born)	IAM-SCAR+I+R
1	27.9	0.9	0.21	27.3	19.6 (10.2)*	56.6	104
1.2	33.1	0.3	0.22	25.3		64.3	
1.5	34.8	1.6	0.22	22.5	13.8 (7.25)*	62.4	85.4
1.7	30.3	0.7	0.27	23.5		63.4	
2	34.8	1.2	0.21	18.9	10.2 (6.33)*	63.1	75.3
2.2	37.8	0.9	0.21	18.0		61.9	
2.5	43.8	1.1	0.22	17.2		60.8	
2.7	46	0.7	0.24	17.3		64.2	
3	50.8	0.9	0.28	17.8	8.74 (8.71)*	66.4	66.9
3.3	48	2.1	0.23	15.3		56.1	

3.6	47.9	0.9	0.22	14.3		51.7	
3.8	44.8	0.9	0.22	13.9		49.9	
4	43.4	1.4	0.23	13.9	6.63 (4.86)	48.6	63.6
4.5	43.2	1.5	0.24	13.3		46.7	
5	47.1	1.1	0.24	12.7	6.03 (4.20)*	46.1	61.0
5.5	47.4	1.6	0.26	12.5		48.7	
6	51.3	0.13	0.24	11.5		49.4	
6.5	47.3	0.9	0.23	10.8		47.3	
7	48.3	1.7	0.26	11.1	5.86 (3.67)*	46.2	59.6
7.5	50.6	1	0.23	10.1		47.1	
8	51.7	1.3	0.2	9.10		49.4	
8.5	55.6	2.1	0.17	8.13		51.0	
9	53.6	1.9	0.27	9.97		53.7	
9.5	54	1.1	0.26	9.52		54.5	
10	58.1	1.6	0.25	9.10	4.96 (3.43)*	53.8	58.2
11	58.3	1	0.25	8.67		57.1	
12	54.6	0.7	0.24	8.13		57.7	
13	61.4	0.8	0.23	7.64		58.1	
14	55.2	0.8	0.24	7.52		58.4	
15	54.8	0.3	0.24	7.27	3.90 (3.43)*	58.4	55.4
16	52.3	0.6	0.21	6.58			
17.5	49.5	1.1	0.27	7.13			
20	49.3	1.1	0.27	6.67	4.14		52.6
25	46.9	1.4	0.19	5.00			

30	47.5	1.8	0.19	4.56	2.66		49.0
40	43.3	1	0.22	4.25	2.07		45.9
50	38.9	0.4	0.22	3.80	2.02		42.8
70	35.4	0.2	0.17	2.82	1.49		38.4
100	33.1	0.3	0.19	2.50	1.38		33.9
150	29.9	1.2	0.21	2.14	0.47		28.6
200	26.9	0.3	0.26	2.07	0.66		25.2
250	22.8	0.8	0.22	1.70			
300	19.8	0.8	0.22	1.55	0.75		20.5

*Calculated with the Born Corrected R-matrix differential cross section values

The absolute random uncertainties listed in Table 1 include the statistical fluctuation of direct measurements and the contribution of the sensitivity limits of all the electronic devices used during the measurement procedure as well as those derived from the numerical data analysis. As the table shows, these uncertainties are within 5 % for all the scattering energies considered. However, we should note here that the main error source linked to transmission experiments such as those presented here is the aforementioned systematic error derived from the energy and angular resolution limits. The energy resolution of the present measurements is shown in Table 1 for each incident electron energy. These values are directly given by the electron intensity distribution of the incident beam as measured with the RPA in combination with the MCP detector (see Ref. 7 for details). As described in Ref. 7, under the present magnetic confinement conditions, the angular resolution ($\Delta\theta$) is determined by the energy resolution (ΔE) according to the following expression:

$$\Delta\theta = \arccos\sqrt{1 - \frac{\Delta E}{E}} \quad (2)$$

The values of $\Delta\theta$ for each incident electron energy are also given in Table 1. Before any comparison between the present experimental data and other available values can be made, an analysis of the energy and angular resolution limitations should be carried out in order to ensure a valid comparison.

In the present measurements the angular and energy resolution limits make it impossible to detect elastically and rotationally scattered (the average rotational excitation energy is less than 1.1 meV) electrons within the $(0-\Delta\theta)$ and $(180-\Delta\theta)$ angular ranges. All these electrons are considered unscattered, thus lowering the measured TCSs. As shown in Ref. 7, the contribution of these “missing angles” ($\sigma(\Delta\theta)$) can be evaluated using the following expression:

$$\sigma(\Delta\theta) = 2\pi \left(\int_0^{\Delta\theta} \frac{d(\sigma_{el} + \sigma_{rot})}{d\Omega} \sin\theta d\theta + \int_{180-\Delta\theta}^{180} \frac{d(\sigma_{el} + \sigma_{rot})}{d\Omega} \sin\theta d\theta \right) \quad (3)$$

By using our IAM-SCAR+I+R and R-matrix-CC-Born differential cross sections (that include, as explained, rotational excitations), the contribution of the “missing angles” to the measured TCSs can be evaluated (MA correction). The results are shown in Table 1. Note that these values always represent a contribution that would increase the observed TCS which may be taken into consideration when comparing with data from other sources.

For energies above 15 eV, where the IAM-SCAR+I+R method applies, there is good agreement (within 8.5%) between the present measurements and the IAM-SCAR+I+R calculation. To illustrate the comparison, the present experimental and theoretical data are plotted in Fig. 1. As can be seen in this figure, if the rotational excitation is not included in the calculation (IAM-SCAR+I values) the agreement between experiment and theory is excellent. This is consistent with the fact that the energy and angular resolution used in most transmission experiments, and in particular the present one, is not good enough to account for the rotational excitation processes and comparisons between experimental and theoretical TCS values should be done excluding dipole rotation calculations. However, at these energies the uncertainty due to the effect of the “missing angles” is less than 8.5%. Combining this source of error with the random uncertainty limits, we consider the present experiment to provide reliable total electron scattering cross sections, within 10%, in the energy range 10-300 eV. The excellent agreement between theory and experiment in this energy range also confirms the validity of introducing interference effects¹⁷ to the independent atom model (IAM) based calculations at intermediate and high energies. Furthermore, as explained in Ref. 17, including the interference term solves the contradiction between the optical theorem and the additivity rule (AR) assumed in such representations.

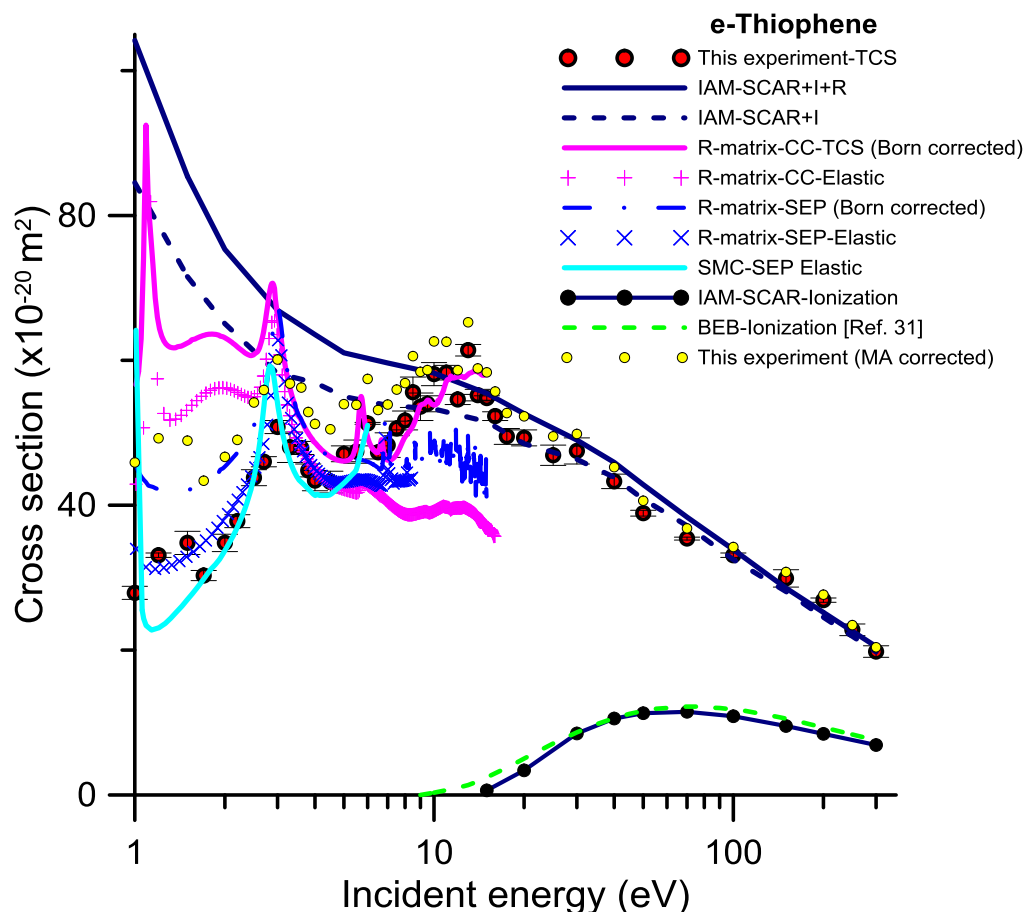


FIG. 1. Total electron scattering cross sections, including the present measurements, our IAM-SCAR+I+R, the R-matrix-SEP and R-matrix-CC with Born correction results together with the R-matrix and SMCPP SEP and R-matrix CC integral elastic cross sections without Born correction. Our IAM-SCAR and the BEB from Ref. 31 ionization cross sections are also shown. See also legend on the figure (color online).

Below 10 eV, the IAM-SCAR+I+R method does not apply and comparison with this method does not make sense. At these lower energies, the comparison should be made with the reliable ab initio R-matrix data. As shown in Table 1, in the 2.1-15 eV energy range we found a good agreement, within 10%, between the experiment (including the “missing angle” correction) and the R-matrix-CC-Born results. Below this energy, from 1 to 2 eV, our calculation tends to give higher cross sections than the experimental values, reaching a maximum discrepancy of about 100% at 1 eV. However, we should note here that the R-matrix-CC-Born calculation includes rotational excitation which are not discernible by the experiment: as expected, these rotational excitations become more relevant for the lower energies. In fact, within the Born approximation the rotational excitation cross sections increase exponentially for decreasing energies. Although we considered our CC the most accurate description of the scattering problem,⁵ Fig.1 shows how our R-matrix-SEP-Born results agree better with the experimental values at these low energies but being still higher than those due to the Born corrected rotational excitations. The dominance of rotational excitations at low energies is illustrated in Fig. 2. Differential elastic and rotational excitation cross sections calculated both with our R-matrix (at the SEP level) and IAM-SCAR+I+R procedures are plotted for 2 eV incident electron energy. The acceptance angle of the detector for this energy is also shown in Fig.2 (dashed black line). The first feature we can distinguish in this figure is that the Born-based procedure used for our R-matrix (the POLYDCS¹⁶ formulation)

and our dipole rotational excitation complementing the IAM-SCAR+I calculations are equivalent, leading to the same contribution to the DCS. As it's also clear, the missing contribution to the cross section due to the acceptance angle limitation comes from the rotational excitation DCS and specifically the Born correction contribution, which are several orders of magnitude higher than the rotationally elastic DCS near 0° . The low energy failure of the IAM-SCAR+I calculation is also clearly explained by the rotationally elastic DCS. While this reproduces reasonably well the angular dependence, its absolute value is much higher (up to 100%) than that given by the R-matrix calculation. However, the predominance of the Born correction at the lower energies justifies the good agreement found, even at very low energies, between both calculations for a highly polar molecule as pyridine.²⁴

The above discussion, shows the usefulness of comparing, for low energies, our experimental TCS with low energy scattering calculations not including the Born correction. Since below 8 eV, (not including rotations) elastic scattering processes are dominant we have included in Fig. 1 our integral elastic (IECS) R-matrix data (both CC and SEP levels)⁵ and the elastic SMCPP⁶ calculation at the SEP level without inclusion of the Born correction. When this correction is excluded (and therefore the contribution of rotational excitation is mostly excluded), the CC-R-matrix IECS are closer, but still higher by about 60%, to the experimental results. However, the SEP R-matrix IECS show a very good agreement with the experimental data. As aforementioned, we have recently considered⁵ our CC approach as the most physical representation of the scattering problem and this is early the case above the first excitation threshold.⁵ However, for very low energies, due to the high molecular polarizability of thiophene (60.8 a_0^3),²⁵ the description of polarisation effects is crucial: it seems clear from Fig. 1 that the polarisation potential used at the SEP levels leads to the best agreement with the experimental results. This is also supported by the excellent agreement between the SMCPP calculation from da Costa et al.⁶ and the present experimental results.

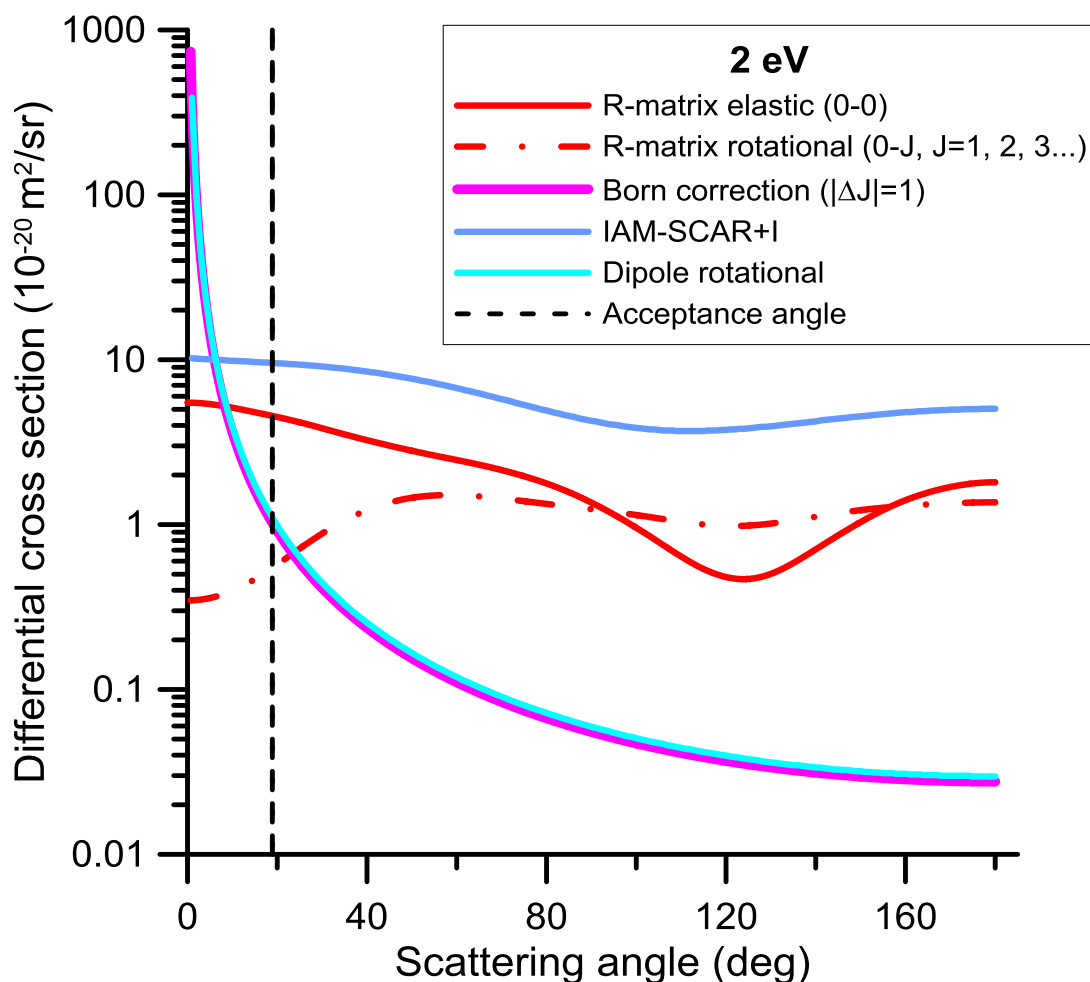


FIG. 2. Calculated differential elastic and rotational excitation cross sections for 2 eV electron incident energy as a function of the scattering angle; the R-matrix data corresponds to the SEP calculation. The acceptance angle of the detector for this incident energy is also shown. See also legend on the figure (color online).

Despite the difficulty involved in the comparison of low energy theoretical and experimental TCS data, this comparison can be very useful to validate some of the resonances predicted by different theories. These resonances appear as enhancement features in the experimental TCS and how well defined they are depends on the energy resolution (about 0.2 eV in this experiment). In the case of thiophene, some of these features are clearly discernible below 15 eV as shown in Fig. 1. As mentioned above, in this energy domain our IAM-SCAR+I calculation does not apply and therefore its results are not going to be considered in this discussion. Both R-matrix⁵ and SMC-SEP⁶ calculation show a well-defined low energy resonance around 1 eV. da Costa et al.⁶ identified this peak as a π^* shape resonance in the B_1 symmetry and their SEP calculation placed it at 1 eV. Our CC R-matrix calculation found a resonance at 1.1 eV, 20% higher than the SEP approach.⁶ Our experimental TCS (see Fig. 1) shows a weak structure around 1.3 ± 0.2 eV. Unfortunately, the energy resolution is not good enough to discriminate between calculations but seems more compatible with a resonance at 1.1 than 1.0 eV where our experimental results present a minimum. This is consistent with our statement that the CC calculation corresponds to the most complete representation of the scattering problem. The second peak, assigned by da Costa et al.⁶ to a superposition of a π^* in the A_2 symmetry and a

σ^* shape resonance in the B_2 symmetry, is located at 2.82 eV in their SEP calculation.⁶ The recent R-matrix analysis of Loupas et al.²⁶ located these resonances at 2.990 eV, the $\sigma^*(B_2)$, and 2.993 eV, the $\pi^*(A_2)$. Other R-matrix based calculation from Vinodkumar et al.²⁷ located the $\sigma^*(B_2)$ resonance at 2.51 eV. These values agree with the present experimental results which present a local maximum of the TCS at 3.0 ± 0.2 eV. The position of these resonances as determined by our experiment is also consistent with the experimental vertical attachment energies of 1.15 and 2.63 eV, respectively, measured by Modelli and Burrow.²⁸

Our experimental TCS values also show an increment around 3.3 ± 0.2 eV which may correspond to that observed by Muftakhov et al.²⁹ at 3.5 eV, attributed by them to a Feshbach-type resonance whose parent state is the first excited triplet state of thiophene (3B_2). Core-excited resonances in thiophene have also been analysed by Loupas et al.²⁶ by comparing the R-matrix calculation with experimental energy loss spectra. The two lowest lying they found were identified as 1^2A_2 at 5.695 eV and 1^2B_1 at 6.70 eV, respectively. The R-matrix calculation from Ref.27 found the 1^2A_2 resonance at 4.77 eV. Measurements of Ref. 29 observed that resonance at 5.3 eV. Our experimental TCS shows a shoulder around 5 eV and a local maximum between 5.5 and 6.5 which is compatible with the position of these resonances when our energy resolution is taken into consideration. Experimental data from Ref. 29 and unpublished measurements cited in Ref. 26 (see Ref.13 in Ref. 26) placed these resonances at 5.3, 5.38, 6.4 and 6.22 eV, respectively, in excellent agreement with the present measurements. In the energy range 6.9-9.5 eV, Loupas et al.²⁶ identify 8 additional resonances. Only for two of them (a 2^2B_1 at 7.96 eV and a 2^2A_2 at 9.22 eV) was any experimental evidence found, although discrepancies on the position of the latter are about 15%. In this energy range, our experimental results only show a local maximum at 8.5 eV. This could be interpreted as a combination of the 2^2B_1 resonance at 7.96 eV (1.2 eV width) with the 2^2A_2 resonance at 9.22 eV (0.95 eV width) which are probably not well resolved by our experimental apparatus. The 8.5 eV resonance was also observed by Muftakhov et al.²⁹ and identified as 2^2A_2 . The present experimental results finally show a broad maximum on the TCS values between 9.5 and 15 eV presenting a weak peak at 11 eV and the absolute maximum value at 13 eV. This broad structure may be related to the excitation of the great number of accessible states, even those from the continuum (the ionisation threshold is 8.86 eV) and the overlap of numerous weak resonances not described by our methods. Above 15 eV it presents a weak shoulder in the range 20-30 eV, probably a consequence of the combination between the decreasing elastic cross section with the still increasing excitation function of the mentioned excited states, and then monotonically decreases according to the energy dependence predicted by the IAM-SCAR+I theory. To summarize this comparison, theoretical and experimental values of the positions of the above resonances are shown in Table 2. Theoretical data from Kossoki and Bettega³⁰ complementing those from Ref. 6 are also included in this table.

Table 2. Position of the resonances observed in this study and those identified in previous experimental and theoretical publications.

Resonance	Experimental position (eV)	Calculated position (eV)
$\pi_1^*(B_1)$	$1.3 \pm 0.2^*$ 1.15 ²⁷	0.949 ²⁶ (SEP) 0.80 ²⁶ (SEP) 1.114 ²⁶ (CC) 1.00 ^{6,30}

$\sigma^*(B_2)$		2.990 ²⁶ (SEP) 2.51 ²⁶ (SEP) 1.5 ²⁶ (CC) 2.78 ^{6,30} 2.51 ²⁷
$\pi_2^*(A_2)$	3.0 ± 0.2* 2.63 ²⁸	2.993 ^d (SEP 35VO) 2.87 ^d (SEP 41VO) 2.909 ^d (CC) 2.82 ^{6,30}
1^3B_2	3.3 ± 0.2* 3.5 ²⁹	
1^2A_2	5.0 ± 0.2* 5.3 ²⁹ 5.38 [†]	4.77 ²⁷ 5.695 ²⁶
1^2B_1	6.0 ± 0.2* 6.4 ²⁹ 6.22 [†]	6.70 ²⁶
1^2B_2		6.9 ²⁶
2^2B_2		7.72 ²⁶
1^2A_1		7.87 ²⁶
2^2B_1	8.5 ± 0.2* 7.39 [†]	7.96 ²⁶
3^2B_2		8.98 ²⁶
3^2B_1		9.01 ²⁶
2^2A_2	8.5 ± 0.2* 8.5 ²⁹ 7.93 [†]	9.22 ²⁶
2^2A_1		9.48 ²⁶

*Present experiment

† Unpublished data (see Ref. 13 in Ref. 26)

Finally, we also present in Fig.1 the ionization cross sections we derived from the IAM-SCAR integral inelastic cross section (see Fig. 4 in Ref.5) by using the alternate absorption threshold procedure mentioned in Section III (see Refs. 22, 23 for details). Electron impact ionization cross section of thiophene in the energy range 9-3000 eV were calculated by Mozejko et al.³¹ by using the binary-encounter-Bethe (BEB) model.³² The agreement between both calculations is fairly good except for energies around the ionisation limit where our IAM-SCAR method, due to the used independent atom representation, is not expected to be accurate. There are no experimental data available in the literature to compare these values so we believe they provide a valuable complement for electron scattering databases.

V. CONCLUSIONS

Experimental electron scattering total cross sections for thiophene in the energy range 1-300 eV have been measured for the first time with a magnetically confined electron transmission-beam apparatus. Total random uncertainty limits have been estimated to be within 5 % by including the statistical reproducibility of the measurements and all the uncertainty sources connected to the measuring devices and data analysis procedures. The energy resolution has been measured directly from the transmission intensity distributions and found to be from 0.17 to 0.28 eV, depending on the incident electron energy. Systematic errors due to electrons elastically and rotationally scattered into the acceptance angle of the detector have been discussed in detail and evaluated with the help of calculated DCS values. Since the average rotational excitation energy of thiophene (about 0.001 eV) is much lower than the present energy resolution and the rotational excitation DCS are strongly peaked in the forward direction, the present experimental TCS data do not in practice account for the rotational excitation processes. Therefore, looking at theoretical results without including Born corrections or dipole Born rotational excitation channels provides a more 'like-with-like' comparison. When this is done, considering the mentioned random uncertainty limits and the angular limitations of the present experimental conditions, good agreement between the present measurements and our IAM-SCAR+I calculation has been found for energies above 15 eV. Below this value, excellent agreement has been found between the present experimental data and our R-matrix calculation at the CC level for energies between 3.6 and 15 eV. For lower energies, the dominant IECS has found to be extremely sensitive to the polarisation treatment included in the calculation procedure. Below these energies, even though the CC level can be considered the most complete representation of the scattering problem we have found the experimental data to be in better agreement with calculations at the SEP level. With respect to the resonance positions, the present measurements confirmed the well-known low-lying π^* and σ^* shape resonances. Although most of the core-excited resonances identified in Ref. 26 are compatible with the present measurements, these do not have enough energy resolution to confirm their energy position and widths. One should also note that some of these core-excited resonances may not enhance the elastic cross section significantly and may therefore not be visible in the TCS. We consider the present experimental values together with our previous calculation and those available in the literature constitute a reasonable electron scattering data set in the range 0-300 eV ready to be used for modelling purposes. Future work to improve its accuracy should focus on the lower energy domain, mainly below 4 eV, improving the polarisation treatment in the R-matrix calculations to eliminate the discrepancy between CC and SEP results and on improving the energy resolution of the cross section measurements.

ACKNOWLEDGEMENTS

This experimental study has been partially supported by the Spanish Ministerio de Ciencia, Innovación y Universidades (Project FIS 2016-80440) and the FP7- European Union-ITN (Project 608163-ARGENT). A.I.L. also acknowledges the “Garantía Juvenil” grant programme from MINECO and support from the Doctorate Program in Science from the UNED University. JDG acknowledges EPSRC funding.

- ¹A. G. Sanz, M. C. Fuss, A. Muñoz; F. Blanco, P. Limão-Vieira, M. J. Brunger, S. J. Buckman and G. García, *Int. J. Rad. Biol.* **88**, 71 (2012).
- ²H. Nikjoo, D. Emfietzoglou, T. Liamsuwan, R. Taleei, D. Liljequist, and S Uehara, *Rep. Prog. Phys.* **79**, 116601 (2016).
- ³R. D. White, D. Cooks, G. Boyle, M. Casey, N. Garland, D. Konovalov, B. Philippa, P. Stokes, J. de Urquijo, O. González-Magaña, R. P. McEachran, S. J. Buckman, M. J. Brunger, G. García, S. Dujko, and Z. Lj. Petrovic, *Plasma Sources Sci. Technol.* **27**, 053001 (2018).
- ⁴Y. Zheng and L. Sanche, *Appl. Phys. Rev.* **5**, 021302 (2018).
- ⁵A. Loupas, A. I. Lozano, J. D. Gorfinkiel and G. García, *J. Chem. Phys.* **149**, 034304 (2018).
- ⁶R. da Costa, M. do N. Varella, M. Lima and M. Bettega, *J. Chem. Phys.* **138**, 194306 (2013).
- ⁷A. I. Lozano, J. C. Oller, K. Krupa, P. Limão-Vieira, F. Blanco, A. Muñoz, R. Colmenares and G. García, *Rev. Sci. Instrum.* **89**, 063105 (2018).
- ⁸M. C. Fuss, A. G. Sanz, F. Blanco, J. C. Oller, P. Limão-Vieira, M. J. Brunger and G. García, *Phys. Rev. A* **88**, 042702 (2013).
- ⁹A. G. Sanz, M. C. Fuss, F. Blanco, J. D. Gorfinkiel, A. Almeida, F. Ferreira da Silva, P. Limão-Vieira, M. J. Brunger and G. García, *J. Chem. Phys.* **139**, 184310 (2013).
- ¹⁰A. McClellan, *Tables of experimental dipole moments* (W.H.Freeman, 1963).
- ¹¹C. Szymtkowski and K. Maciag, *Phys. Script.* **54**, 271 (1996).
- ¹²Y. Itikawa, *J. Phys. Chem. Ref. Data* **35**, 31 (2006).
- ¹³J. Tennyson, *Phys. Rep.* **491**, 29(2010).
- ¹⁴P. G. Burke, *R-Matrix Theory of Atomic Collisions: Application to Atomic, Molecular and Optical Processes* (Springer, 2011).
- ¹⁵J. M. Carr, P. G. Galiatsatos, J. D. Gorfinkiel, A. G. Harvey, M. A. Lysaght, D. Madden, Z. Mašín, M. Plummer, J. Tennyson, and H. N. Varambhia, *Eur. Phys. J. D* **66**, 20653 (2012).
- ¹⁶N. Sanna and F. Gianturco, *Comput. Phys. Commun.* **114**, 142 (1998).
- ¹⁷F. Blanco, L. Ellis-Gibbins and G. García, *Chem. Phys. Lett.* **645**, 71 (2016).
- ¹⁸A. G. Sanz, M. C. Fuss, F. Blanco, F. Sebastianelli, F. A. Gianturco, and G. García, *J. Chem. Phys.* **137**, 124103 (2012).
- ¹⁹A. Traoré Dubuis, F. Costa, F. Ferreira da Silva, P. Limão-Vieira, J. C. Oller, F. Blanco and G. García, *Chem. Phys. Lett.* **699**, 182 (2018).
- ²⁰N. Hishiyama, M. Hoshino, F. Blanco, G. García and H. Tanaka, *J. Chem. Phys.* **147**, 224308 (2017).
- ²¹F. Blanco, F. Ferreira da Silva, P. Limão-Vieira and G. García, *Plasma Sources Sci. Technol.* **26**, 085004 (2017).
- ²²W. A. D. Pires, K. L. Nixon, S. Ghosh, R. F. C. Neves, H. V. Duque, R. A. R. Amorim, D. B. Jones, F. Blanco, G. García, M. J. Brunger and M. C. A. Lopes, *Int. J. Mass Spectrom.* **422**, 32 (2017).
- ²³S. Ghosh, K. L. Nixon, W. A. D. Pires, R. A. R. Amorim, R. F. C. Neves, H. V. Duque, M. G. M. da Silva, D. B. Jones, F. Blanco, G. García, M. J. Brunger and M. C. A. Lopes, *Int. J. Mass Spectrom.* **430**, 44 (2018).
- ²⁴A. Sieradzka, F. Blanco, M. C. Fuss, Z. Mašín, J. D. Gorfinkiel, and G. García, *J. Phys. Chem. A* **118**, 6657 (2017).

- ²⁵ R. D. J. I. Editor, "Nist standard reference database," <http://http://cccbdb.nist.gov>, accessed: 2017-10-04.
- ²⁶ A. Loupas, K. Regeta, M. Allan and J. D. Gorfinkiel, *J. Phys. Chem. A* **122**, 1146 (2018).
- ²⁷ M. Vinodkumar, H. Desai, P. C. Vinokudmar, *RSC Adv.* **5**, 69466 (2015).
- ²⁸ A. Modelli and P. D. Burrow, *J. Phys. Chem. A* **108**, 5721 (2004).
- ²⁹ M. V. Muftakhov, N. L. Asfandiarov, and V. I. Khvostenko, *J. Electron Spectrosc. Relat. Phenom.* **69**, 165 (1994).
- ³⁰ F. Kossoki and M. H. F. Bettega, *J. Chem. Phys.* **138**, 234311 (2013).
- ³¹ P. Możejko, E. Ptasińska-Denga, and Cz. Szmytkowski, *Eur. Phys. J. D*, **66**, 44 (2012).
- ³² W. Hwang, Y.-K. Kim, and M.E. Rudd, *J. Chem. Phys.* **104**, 2956 (1996).

Lista completa de publicaciones

1. **A. I. Lozano**, J. C. Oller, D. B. Jones, R. F. da Costa, M. T. do N. Varella, M. H. Bettega, F. Ferreira da Silva, P. Limão-Viera, M. A. P. Lima, R. D. White, M. J. Brunger, F. Blanco, A. Muñoz, and G. García. "Total electron scattering cross sections from *para*-benzoquinone in the energy range 1-200 eV", Phys. Chem. Chem. Phys., **20**, 22368 (2018). DOI: 10.1039/c8cp03297a
2. **A. I. Lozano**, A. Loupas, F. Blanco, J. D. Gorfinkield, and G. García. "Total electron scattering cross sections from thiophene for the (1-300 eV) impact energy range". J. Chem. Phys. **149**, 134303 (2018). DOI: 10.1063/1.5050349
3. A. Loupas, **A. I. Lozano**, F. Blanco, J. D. Gorfinkield, and G. García. "Cross sections for electron scattering from thiophene for a broad energy range". J. Chem. Phys. **149**, 034304 (2018). DOI: 10.1063/1.5040352
4. **A. I. Lozano**, J. Jiménez, F. Blanco, and G. García. "Total electron-scattering cross section from pyridine in the energy range 1 -200 eV". Phys. Rev. A **98**, 012709 (2018). DOI: 10.1103/PhysRevA.98.012709
5. **A. I. Lozano**, F. Ferreira da Silva, F. Blanco, P. Limão-Vieira, and G. García. "Total electron scattering cross section from sevoflurane by 1 – 300 eV energy electron impact". Chem. Phys. Lett. **706** (2018). DOI: 10.1016/j.cplett.2018.07.005
6. **A. I. Lozano**, J. C. Oller, K. Krupa, F. Ferreira da Silva, P. Limão-Vieira, F. Blanco, A. Muñoz, R. Colmenares, and G. García. "Magnetically confined electron beam system for high resolution electron transmission-beam experiments". Rev. Sci. Instrum. **89**, 063105 (2018). DOI: 10.1036/1.5030068
7. **A. I. Lozano**, K. Krupa, F. Ferreira da Silva, P. Limão-Vieira, F. Blanco, A. Muñoz, D. B. Jones, M. J. Brunger, and G. García. "Low energy electron transport in furfural". Eur. Phys. J. D **71**, 226 (2017). DOI: 10.1140/epjd/e2017-80326-0
8. **A. I. Lozano**, L. Álvarez, F. Blanco, M. J. Brunger, and G. García. "Total cross section measurements for electron scattering from dichloromethane". J. Chem. Phys. (sometido a publicación)